Title:

Small RNA-mediated genomic silencing promotes telomere stability in the absence of telomerase

Authors:

Charlie Longtine[1,2,#], Stephen Frenk[1,2,#], and Shawn Ahmed[1,2]*

Affiliations:

[1]Department of Genetics, [2]Department of Biology, University of North Carolina, Chapel Hill, NC, USA

# Equal contributions
*Correspondence and Lead Contact: shawn@med.unc.edu

Short title: small RNAs promote telomere stability

Abstract

Telomerase deficiency in human somatic cells results in telomere erosion and senescence. Small RNAs that target telomeres have been observed in diverse organisms but their functions are not well characterized. We define an endogenous small RNA pathway in *Caenorhabditis elegans* that promotes heterochromatin formation at telomeres via Dicer, the perinuclear Argonaute protein WAGO-1 and the nuclear Argonaute protein HRDE-1. Loss of telomerase induces biogenesis of siRNAs that target the telomeric lncRNA TERRA, whereas loss of both telomerase and small RNA-mediated telomeric silencing induces TERRA expression, DNA damage, and an accelerated sterility phenotype. These phenotypes can be rescued by exogenous telomeric siRNAs or by loss of the DNA damage response protein EXO-1. Thus, endogenous siRNAs interact with TERRA to promote heterochromatin formation in a manner that is critical for the stability of naturally eroding telomeres. We propose that small RNA-mediated genome silencing could be broadly relevant to regulation of proliferative aging.

Introduction

Telomeres are repetitive nucleoprotein structures that protect the ends of linear eukaryotic chromosomes from degradation and recognition as double-stranded DNA breaks (Maciejowski and de Lange, 2017, Shay, 2016). In most human somatic cells, which are deficient for telomerase reverse transcriptase, telomeres erode over progressive cell divisions, eventually triggering replicative senescence (Holohan et al., 2014, Shay, 2016). Telomere shortening thus acts as a barrier to tumorigenesis, but may also contribute to organismal aging through impaired stem cell function, regeneration, and organ maintenance (Donate and Blasco, 2011, Shay, 2016). Regulating the rate of telomere erosion in telomerase-negative cells is therefore crucial to maintain this balance between tumor suppression and age-related tissue decline (Li et al., 2017, Maciejowski and de Lange, 2017). Tumor cells escape telomere-triggered senescence by stabilizing telomere length, either through reactivation of telomerase or through activation of the telomerase-independent recombination-mediated telomere

maintenance pathway termed Alternative Lengthening of Telomeres (ALT) (Pickett and Reddel, 2015).

Telomeres have features characteristic of heterochromatin in that they associate with the heterochromatin protein HP1 and contain transcriptionally repressive histone marks such as methylation of H3K9 and H4K20 (Benetti et al., 2007, McMurchy et al., 2017). Nonetheless, telomeres are transcribed into the G-rich long noncoding RNA (lncRNA) termed TERRA, a feature widely conserved among eukaryotes, and lower levels of the C-rich antisense lncRNA ARRET have also been reported (Azzalin et al., 2007). TERRA is transcribed from the subtelomere into the telomere by RNA polymerase II and is upregulated at shortened and damaged telomeres, where it may recruit telomerase and chromatin modifiers to promote telomere elongation (Azzalin and Lingner, 2015, Cusanelli et al., 2013). Telomere elongation represses expression of TERRA through increased methylation and HP1 binding (Arnoult et al., 2012). Notably, telomere shortening in mice with telomerase defects and overexpression of a negative regulator of telomere length have been associated with loss of heterochromatic marks at telomeres and subtelomeres (Benetti et al., 2007, Benetti et al., 2008).

Transcriptional silencing and heterochromatin deposition at repetitive segments of the genome such as the pericentromere (Holoch and Moazed, 2015, Reinhart and Bartel, 2002) require long non-coding RNA (lncRNA) transcripts that promote biogenesis of and interact with small RNAs that direct heterochromatin factors to target genomic loci. Endogenous sources of double-stranded RNA such as sense-antisense transcript hybrids can be processed into small RNAs that play roles in creating and maintaining siRNA-mediated heterochromatin, where paradoxically RNA expression is required for genomic silencing. Bidirectional transcription of telomeres has been linked to production of telomeric siRNAs that promote subtelomeric DNA methylation in *Arabidopsis* (Vrbsky et al., 2010). The presence of similar telomeric siRNAs has also been observed in *Tetrahymena*, mouse stem cells, and human cell lines (Cao et al., 2009, Rossiello et al., 2017), but their functional relevance at canonical telomeres is not well understood in any experimental system.

102

103 Germline transcription in *C. elegans* is regulated in part by a network of small RNA
104 pathways that promote silencing or expression of target loci in a sequence-specific
105 manner (Billi et al., 2014). Transcription of potentially harmful foreign genetic elements
106 including transposons and transgenes is repressed by 21 nucleotide PIWI-interacting
107 RNAs or piRNAs. These interact with PRG-1, a member of the PIWI clade of Argonaute
108 proteins that recognizes RNA targets of piRNAs based on sequence complimentarity
109 with up to 3 mismatches (Bagijn et al., 2012, Batista et al., 2008, Das et al., 2008). RNA
110 target recognition triggers the recruitment of RNA-dependent RNA polymerases
111 (RdRPs) that act in Mutator bodies, which are associated with perinuclear P granules, to
112 create *de novo* 22 nucleotide secondary siRNAs with a 5' guanine (22G RNAs) (Pak
113 and Fire, 2007). These 22G RNAs are loaded onto worm-specific Argonaute proteins
114 (WAGOs) such as the nuclear WAGO HRDE-1, which promotes heterochromatin
115 deposition at target loci (Ashe et al., 2012, Buckley et al., 2012). Germline transcription
116 is protected by a separate set of 22G RNAs that interact with the anti-silencing
117 Argonaute protein CSR-1 (Avgousti et al., 2012, Wedeles et al., 2013) . Aside from the
118 piRNA pathway, 22G activity can be triggered by primary siRNAs from other sources.
119 For example, DCR-1, the *C. elegans* homologue of the highly conserved RNAse class
120 III enzyme Dicer, can cleave endogenous and exogenous double stranded RNA
121 transcripts to create primary 26G RNAs, which bind a distinct set of Argonautes to
122 trigger target silencing through the 22G pathway described above (Bernstein et al.,
123 2001, Ketting et al., 2001, Knight and Bass, 2001).
124

125 Here we describe an endogenous siRNA pathway that represses TERRA via
126 heterochromatin formation and functions redundantly with telomerase to promote
127 telomere stability.
128

129 **Results**
130

131 **Loss of endogenous siRNAs or XNP-1/ATRX does not promote ALT**

High levels of TERRA and loss of the histone H3.3 chaperone subunits ATRX and DAXX commonly occur in human ALT cancers (Flynn et al., 2015, Lovejoy et al., 2012). The ATRX/DAXX complex mediates histone H3.3 incorporation at telomeres and interacts with methylated H3K9 and HP1 to promote heterochromatin formation (Wong et al., 2010), which has been proposed to repress ALT by protecting telomeres from replication stress and TERRA expression (Udugama et al., 2015). We have previously shown that 10-20% of *C. elegans* strains that are deficient for telomerase can be maintained indefinitely through the activation of ALT (Cheng et al., 2012). Because human ALT cancers are characterized by ATRX-mediated heterochromatin dysfunction, we reasoned that small RNA factors that promote heterochromatin silencing might regulate the establishment of ALT. We tested this hypothesis by passaging *trt-1* telomerase mutant strains that were deficient for biogenesis of either primary or secondary siRNAs by transferring 100s of worms per strain weekly, which reliably allows survival of 10-20% of strains via ALT (Cheng et al., 2012). Loss of either primary siRNAs (*trt-1; dcr-1)* or downstream secondary siRNAs (*trt-1; mut-7* and *trt-1; mut-14)* did not significantly alter the proportion of strains that survive via ALT (Figure 1A, Table S1). Similarly, loss of the histone H3.3 chaperone XNP-1/ATRX itself did not affect the establishment or maintenance of ALT (Table S1), indicating that loss of neither siRNA- nor XNP-1/ATRX-mediated heterochromatin formation is sufficient to promote ALT.

Small RNA and heterochromatin factors repress rapid sterility when telomerase is deficient

C. elegans strains mutant for telomerase reverse transcriptase, *trt-1,* become uniformly progressively sterile – analogous to crisis that is induced by telomere erosion, chromosome fusion and genome catastrophe in checkpoint-deficient telomerase-negative mammalian cells – when 6 worms are passaged weekly (Ahmed and Hodgkin, 2000), which eliminates survival via ALT (Cheng et al., 2012). Intriguingly, when passaged by transferring 6 L1 larvae per week, *trt-1* mutant lines lacking primary or secondary siRNA biogenesis factors became sterile significantly faster than *trt-1* single mutants (Figure 1B, Table S2). siRNA-deficient *trt-1* strains rapidly accumulated end-to-end chromosome fusions by generation F12, a characteristic of telomerase mutants

163 that have grown for more than 20 generations (Figure 1G). These strains also displayed
164 high levels of DNA damage by generation F6 that were not observed for *trt-1* single
165 mutant controls (Figure 1H). As oocyte karyotypes can only reliably detect the
166 presence of multiple chromosome fusions, we performed genetic crosses that would be
167 capable of detecting a single heterozygous end-to-end chromosome fusion (Ahmed and
168 Hodgkin, 2000). Chromosome fusions cause non-disjunction events during meiosis that
169 elicit dominant embryonic lethality or X0 male phenotypes in progeny of heterozygous
170 F1 animals. We crossed four independent *trt-1 dcr-1* F4 hermaphrodites and failed to
171 detect fused chromosomes that were present in generation F24 *trt-1* mutant controls (p
172 = 3.841e-05 for males and p = 3.61e-05 for dead embryos, Mann Whitney U test) (Table
173 S3). Together, these results suggest that loss of small RNAs and telomerase elicits
174 telomere damage but not telomere fusions in early generations, and that the rapid
175 sterility of these strains in later generations is promoted by critically shortened
176 telomeres that give rise to abundant end-to-end chromosome fusions. Small RNA
177 factors required to prevent this accelerated sterility included RDE-4, which binds
178 endogenous dsRNA and forms a complex with the Dicer nuclease DCR-1, and the
179 Argonaute RDE-1, which acts with the RNA-dependent RNA polymerase RRF-3 to
180 promote production of dsRNA-derived primary siRNAs (Gent et al., 2010, Steiner et al.,
181 2009, Tabara et al., 2002) (Figure 1B). The MUTATOR proteins MUT-7 and MUT-14,
182 which also were required to prevent rapid sterility in *trt-1* (Figure 1B), promote
183 amplification of 22G secondary siRNAs that act as downstream effector siRNAs by
184 promoting mRNA degradation in the cytoplasm or transcriptional silencing in the
185 nucleus (Billi et al., 2014, Ketting et al., 1999, Tijsterman et al., 2002).
186
187 Southern blotting suggested that *dcr-1* and *mut-14* single mutants do not have shorter
188 telomeres than wildtype or *trt-1* mutant strains (Figure S1), which implies that the
189 accelerated sterility of small RNA-deficient *trt-1* mutant strains is unlikely to be a
190 consequence of short telomeres that are inherited from gametes of small RNA-deficient
191 grandparents. We tested this premise using genetics, by crossing a *trt-1; dcr-1* double
192 mutant hermaphrodite with *dcr-1* mutant males, singling *trt-1 +/-; dcr-1 -/-* F1
193 hermaphrodites and isolating *trt-1; dcr-1* double mutant F2. This cross was repeated 15

194 times, to create a *trt-1; dcr-1* double mutant strain whose telomeres should be
195 exclusively derived from the *dcr-1* mutant background. The *trt-1; dcr-1* 15x strain
196 became sterile slightly more slowly than freshly created *trt-1; dcr-1* double mutants (p =
197 0.07) (Fig. 1H), indicating that shortened telomeres transmitted from the *dcr-1* mutant
198 cannot explain the rapid sterility of *trt-1; dcr-1* double mutants. Because none of the
199 small RNA single mutants tested became progressively sterile or accumulated
200 chromosome fusions (Figure 1G), we conclude that telomere maintenance is not
201 impaired in small RNA-deficient lines in the presence of telomerase. We analyzed the
202 dynamics of telomere erosion using terminal restriction fragment analysis, but did not
203 observe an obvious difference between *trt-1* and siRNA-deficient *trt-1* mutant strains
204 (Figure S2). Two other small RNA factors, RRF-2 and ERI-1, were not required to
205 prevent rapid onset of sterility, indicating that the endogenous siRNA pathway that
206 requires ERI-1 (Gent et al., 2010, Han et al., 2009) is dispensable for telomere
207 protection in the absence of telomerase (Figure 1B).
208
209 We hypothesized that small RNAs might repress rapid sterility by directing chromatin
210 factors to telomeres to promote deposition of heterochromatic marks. *C. elegans*
211 telomeres have previously been reported to be enriched for H3K9me2 and bound by the
212 HP1 homolog HPL-2, which promotes H3K9me2 deposition and heterochromatin
213 formation, but not by the other *C. elegans* HP1 homolog HPL-1, which interacts with
214 H3K9me3 (Canzio et al., 2014, McMurchy et al., 2017). We confirmed that H3K9me2
215 but not H3K9me3 was enriched at *C. elegans* telomeres using high throughput
216 sequencing data sets generated from chromatin immunoprecipitation (ChIP)
217 experiments performed by independent groups (McMurchy et al., 2017, Zeller et al.,
218 2016). Moreover, we observed small H3K9me2 domains that extended into the
219 subtelomere at all twelve *C. elegans* chromosome ends (Figure 3A-D). H3K4
220 methylation, which is associated with regions of active transcription, must be removed
221 by demethylases prior to deposition of repressive H3K9 methylation (Greer et al., 2010,
222 Li et al., 2008). Similar to primary and secondary siRNA-deficient *trt-1* strains, loss of
223 HPL-2 but not HPL-1, and loss of either of the two *C. elegans* H3K4 demethylases
224 RBR-2/KDM5 or SPR-5/LSD1, caused accelerated senescence in *trt-1* mutants (Figure

225 1C). Thus, H3K4 demethylation and H3K9me2 deposition prevent telomere instability in
226 the absence of telomerase.
227
228 The histone remodeling protein XNP-1/ATRX has previously been implicated in
229 telomeric heterochromatin formation and interacts with unmethylated H3K4 and
230 methylated H3K9 deposited on the histone variant H3.3 (Udugama et al., 2015). *trt-1*
231 *xnp-1* double mutants went sterile significantly faster than *trt-1* single mutants but not as
232 fast as small RNA deficient *trt-1; mut-7* double mutants (Figure 1D). This suggests that
233 XNP-1 may mediate some, but not all heterochromatin formation at telomeres, possibly
234 because siRNA-dependent methylation of histones other than H3.3, such as canonical
235 histone H3 or H4 can promote telomere stability. Additionally, because loss of both
236 XNP-1 and MUT-7 did not cause an additive effect on survival in *trt-1* mutant strains
237 (Figure 1D), these genes may function in the same pathway, which implies that siRNAs
238 direct the chromatin remodeler XNP-1 to telomeres to repress rapid sterility in the
239 absence of telomerase.
240
241 **Increased expression of TERRA in small RNA and chromatin deficient *trt-1* strains**
242 We hypothesized that DCR-1 and RDE-4 may interact with telomeric dsRNA produced
243 from bidirectional transcription of telomeres into TERRA and ARRET, to create primary
244 siRNAs that are then amplified into a secondary siRNA population that triggers small
245 RNA-dependent silencing of TERRA (Rossiello et al., 2017, Vrbsky et al., 2010). To
246 test whether small RNA and chromatin factors regulate telomeric transcription we
247 measured the abundance of TERRA by qRT-PCR at three chromosome ends using
248 primers within their H3K9me2-coated subtelomere domains (Figure 3A-D). Compared
249 to *trt-1* single mutant controls, TERRA was upregulated in early-generation *trt-1; rde-4*,
250 and *trt-1; mut-14* and *trt-1; spr-5* double mutants (Figure 2A). These high levels of
251 TERRA transcription were markedly induced in small RNA and heterochromatin
252 mutants that lacked telomerase, consistent with the hypothesis that TERRA
253 transcription is specifically induced at damaged or shortened telomeres (Porro et al.,
254 2014, Rossiello et al., 2017).
255

256 We next used RNA Fluorescence *In Situ* Hybridization (FISH) to confirm the effects on
257 TERRA expression and to examine its cell and tissue localization. In wildtype control
258 and *trt-1* mutant hermaphrodite and male worms, TERRA was expressed at low levels
259 in the soma as well as the pachytene region of the meiotic germline (Figures 2B-D, S3-
260 4), which corresponds to the location of several lncRNA-mediated germline silencing
261 processes (Taylor et al., 2015), including Meiotic Silencing of Sex Chromosomes in
262 mammals and *C. elegans* (Heard and Turner, 2011) and a transcriptional burst of
263 piRNAs in mammals that primes genomic silencing in germ cells prior to gametogenesis
264 (Gou et al., 2014). Compared to both wildtype control and *trt-1* or *dcr-1* single mutant
265 strains, *trt-1; dcr-1* double mutant strains had increased expression of TERRA in the
266 germline (Figures 2B-D, S3) and soma (Figures S3-4) by the F6 generation.
267 Endogenous siRNAs thus regulate telomeric transcription in both the soma and
268 germline during telomere attrition, likely through the production of siRNAs that directly
269 target the heterochromatin factors HPL-2, RBR-2 and SPR-5 to telomeres.
270
271 **Subtelomeric siRNAs are upregulated in telomerase mutants**
272 Telomeric siRNAs have been observed in protists, plants and mammals (Cao et al.,
273 2009, Vrbsky et al., 2010). We therefore interrogated 92 publicly available small RNA
274 sequencing libraries created from RNA isolated from various *C. elegans* strains (Fischer
275 et al., 2011, Gent et al., 2010, Gu et al., 2009, Phillips et al., 2015, Phillips et al., 2014,
276 Sapetschnig et al., 2015, Seth et al., 2013) and found rare reads that mapped perfectly
277 to the *C. elegans* telomere repeat $(TTAGGC)_n$, occurring at a frequency of 1 per
278 10,000,000 reads. piRNAs with up to 3 mismatches can target regions of the *C. elegans*
279 genome for silencing (Bagijn *et al.*, 2012) , and we found that telomeric siRNAs with up
280 to 3 mismatches were substantially more abundant than those with perfect telomere
281 repeat sequence (1 per 100,000). Telomeric siRNAs with zero to two mismatches were
282 significantly more likely to be composed of the telomeric G-strand sequence than would
283 be expected by chance ($p < 2.2e-16$, binomial test) (Figure 3E). The proportion of
284 telomeric siRNAs with one or two mismatches beginning with a G nucleotide was
285 significantly greater than that for all mappable reads ($p < 1e-15$, Fisher's exact test) and
286 the median length for these RNAs was 22 nucleotides (Figure 3D, F), suggesting that

287 telomeric siRNAs mapping imperfectly to telomeres are enriched for 22G RNA species.
288 This is consistent with the model that primary siRNAs recruit RNA-dependent RNA
289 polymerases to target RNAs in order to create secondary effector siRNA populations de
290 novo that are highly enriched for 22G RNAs (Gu et al., 2009). We compared levels of
291 telomeric siRNAs from wild-type with those of small RNA mutants that promote telomere
292 stability in the absence of telomerase, such as *dcr-1*, *rde-4*, *mut-7*, *mut-14*, and found
293 that levels of telomeric siRNAs were sometimes depleted in these backgrounds, but not
294 always (File S1).
295
296 Given that telomeric siRNAs are rare in small RNA sequencing data sets, we
297 hypothesized that loss of telomerase might elicit production of telomeric siRNAs in a
298 manner that might depend on Dicer. We therefore isolated RNA from wildtype control,
299 *trt-1* single mutant, and *trt-1; dcr-1* double mutant strains and prepared small RNA
300 libraries. We sequenced these libraries deeply in an effort to detect rare telomeric
301 siRNAs. We obtained ~20,000,000 reads each for 6 data sets and found that our *trt-1*
302 *dcr-1* data sets were strongly depleted of 22G RNAs that were previously reported to
303 depend on *dcr-1* (Figure S5A) (Gent et al., 2010). To assess TRT-1-dependent changes
304 in siRNAs throughout the genome, we counted the number of 22G reads mapping
305 uniquely antisense to protein-coding genes and found upregulation of siRNAs at 720
306 loci and downregulation at 456 loci in *trt-1* animals compared with wild-type (Figure
307 S5B). Of the upregulated loci, 465 were not upregulated in *trt-1; dcr-1* animals
308 compared with wild-type, indicating DCR-1 dependence. We did not find significant GO
309 terms in loci with either up or downregulated siRNA production. Given the importance of
310 both TRT-1 and siRNAs in germline function, we asked whether the loci with differential
311 siRNA production were enriched for germline-enriched genes. We used previously
312 published data on germline expression (Ortiz et al., 2014) and found significant
313 enrichment for germline-enriched genes in both upregulated and downregulated loci (p
314 $< 1e-19$ and $p < 1e-33$ respectively, Pearson's Chi Square test with Bonferroni
315 correction) (Figure S5C). This may reflect a form of epigenome dysregulation within
316 germ cells that occurs as a consequence of telomerase deficiency. siRNAs mapping to

317 transposons were unaffected by loss of TRT-1, with the exception of the CER-10 LTR
318 retrotransposon, for which siRNAs were three-fold downregulated (Figure S5D).
319
320 We detected no siRNAs composed of perfect telomere repeats in any genetic
321 background, but found some with up to 3 mismatches, whose levels did not change
322 substantially in siRNAs from *trt-1* single mutants or *trt-1; dcr-1* double mutants (Figure
323 4A). We next examined 22G RNAs at subtelomeric regions (defined as the 2kb of
324 sequence adjacent to the telomere) and found that these were present in wildtype
325 samples at the left end of chromosome III, and that their abundance was increased two-
326 fold in *trt-1* single mutants and their presence almost entirely eliminated in *trt-1; dcr-1*
327 double mutants (Figure 4C, E). Subtelomeric siRNAs were also observed within 1kb of
328 the telomere at the left ends of chromosomes *I* and *IV* in *trt-1* mutants and not in
329 wildtype or *trt-1; dcr-1* double mutants (Figure 4B, D). The right ends of Chromosomes *I*
330 and *III* and the left end of Chromosome *II* all showed at least a two-fold increase in
331 subtelomeric siRNAs in *trt-1* and/or *trt-1; dcr-1* double mutants (Figure 4E). We
332 observed a significant bias for subtelomeric siRNAs whose sequences correspond to
333 the C-rich telomere strand (antisense to TERRA) for the left arms of Chromosomes *I*
334 and *III* ($p < 1e-13$ and $p < 1e-43$ respectively, binomial test with Bonferroni correction)
335 and for the right arm of Chromosome *I* ($p < 1e-172$, binomial test with Bonferroni
336 correction) while the nucleotide sequences of subtelomeric siRNAs at the left arm of
337 Chromosome *IV* and the right arm of Chromosome *III* showed a bias for subtelomeric
338 TERRA, suggesting that they were created from ARRET ($p < 1e-11$, $p = 0.006$
339 respectively, binomial test with Bonferroni correction) (Figure 4F). These observations
340 suggest that telomere dysfunction triggers the upregulation of small RNA biogenesis at
341 multiple subtelomeres, through both DCR-1-dependent and -independent mechanisms.
342
343 We next studied data sets of small RNAs that immunoprecipitate with HRDE-1 and
344 WAGO-1, Argonaute proteins that promote silencing in the germline, as well as with the
345 germline anti-silencing Argonaute CSR-1 (Table S3). Enrichment of small RNAs for
346 each protein was calculated by dividing the number of reads in the immunoprecipitate
347 library by the number of reads in the corresponding input library. Telomeric siRNAs

348 were enriched in WAGO-1 immunoprecipates relative to input, but this was not the case
349 for HRDE-1 or CSR-1 (Figure 3G). Enrichment of subtelomeric small RNAs in WAGO-1
350 was detected at all chromosome ends tested apart from the right arm of Chromosome *I*
351 (some chromosome ends were not tested due to an absence of reads in the input
352 library). Enrichment was also detected for HRDE-1 at all chromosome ends excluding
353 the right arm of Chromosome *I* and the left arm of Chromosome *III* (Figure 3H).
354 Interestingly, CSR-1 showed the opposite pattern of enrichment to WAGO-1 and HRDE-
355 1, with enrichment at none of the chromosome ends apart from the right end of
356 Chromosome *I*. The ribosomal DNA, the most highly expressed locus in the *C. elegans*
357 genome, is immediately adjacent to this telomere (Wicky et al., 1996), and it is therefore
358 possible that siRNA activity takes a predominantly anti-silencing function at this
359 chromosome end. We asked if either Argonaute that associates with telomeric or sub-
360 telomeric siRNAs, WAGO-1 or to a lesser degree HRDE-1, promotes telomere
361 maintenance in the absence of telomerase and found that both *wago-1 trt-1* and *trt-1;*
362 *hrde-1* double mutants displayed rapid sterility phenotypes in comparison to *trt-1* single
363 mutants ($p < 1e-11$ and $p < 1e-12$, respectively, log rank test) (Figure 1E).
364

365 **Telomeric siRNAs and loss of EXO-1 repress sterility in the absence of**
366 **telomerase**

367 Although we failed to detect siRNAs with perfect telomere repeat sequence in our
368 siRNA data sets, these were present at very low levels in data sets generated by other
369 groups (Figure 3D-F) and could be difficult to detect for technical reasons. We
370 hypothesized that if loss of small RNAs directly targeting the telomere were responsible
371 for the rapid sterility in siRNA-deficient *trt-1*, then reintroduction of exogenous telomeric
372 siRNAs might rescue this phenotype. To address this experimentally, we used a viable
373 *dcr-1* allele, *mg375*, which is deficient for endogenous siRNA production but is
374 hypersensitive to exogenous RNAi when fed *E. coli* expressing dsRNA (Welker et al.,
375 2010). *trt-1; dcr-1(mg375)* double mutants that were passaged on bacteria expressing
376 telomeric dsRNA remained fertile significantly longer than those expressing dsRNA from
377 an empty vector control (Figure 4A). This delay of sterility did not occur for *trt-1* single
378 mutant controls. Moreover, *trt-1; dcr-1(mg375)* strains fed telomeric dsRNA had

379 markedly reduced levels of DNA damage at F6 in comparison to *trt-1; dcr-1(mg375)*
380 strains grown on control RNAi or on regular OP50 bacteria that do not express dsRNA
381 (Figure 1F, 5C).
382
383 In budding yeast, artificially-induced TERRA overexpression promotes telomere
384 shortening *in cis* by forming RNA:DNA hybrids that stall telomeric replication forks as
385 well as by stimulating telomeric resection by Exo1 (Maicher et al., 2012, Pfeiffer and
386 Lingner, 2012). We therefore hypothesized that loss of EXO-1 might rescue the
387 accelerated sterility phenotype in siRNA-deficient telomerase mutants. *trt-1; exo-1;*
388 *mut-14* triple mutant lines survived significantly longer than *trt-1; mut-14* double mutants
389 (Figure 5B) and showed reduced DNA damage and expression of moderate levels of
390 TERRA at F6 (Figures 5B, S5). Moreover, *trt-1; exo-1* double mutant controls remained
391 fertile even longer than *trt-1* single mutants (Figure 5B), indicating that EXO-1-mediated
392 resection promotes telomere-shortening-induced senescence in the absence of
393 telomerase, both at normal telomeres and at telomeres lacking siRNA-mediated
394 silencing. While *trt-1; exo-1* double mutant controls remained fertile longer than *trt-1*
395 single mutants, this was not true for *trt-1* single mutants grown on exogenous telomeric
396 dsRNA (Figure 5A, B). Thus, although loss of *exo-1* rescues the rapid sterility
397 phenotype in small RNA-deficient telomerase mutants, resection by EXO-1 also likely
398 promotes telomere shortening in *trt-1* single mutants independent of siRNA production
399 and telomeric heterochromatin structure.
400
401
402 **Discussion**
403
404 We propose the following model, based in part on our observations: upon telomere
405 shortening or damage, TERRA expression is transiently induced, which may recruit
406 telomerase (Moravec et al., 2016). If telomerase is present, shortened telomeres are
407 elongated. When telomerase is deficient, TERRA expression is suppressed via an
408 endogenous small RNA pathway that interacts with TERRA to facilitate telomeric
409 heterochromatin deposition. We observed upregulation of telomeric and subtelomeric

410 siRNAs in telomerase mutants, which may act as a negative feedback mechanism to
411 maintain appropriate levels of TERRA in the absence of telomerase. H3K9me2 but not
412 H3K9me3 is present at wildtype *C. elegans* telomeres, and we found that the *C.*
413 *elegans* HP1 homolog HPL-2 that binds to and specifically stabilizes H3K9me2
414 (McMurchy et al., 2017) represses telomere instability in the absence of telomerase. We
415 therefore propose that siRNAs function at naturally eroding telomeres to promote
416 heterochromatin formation in a manner that suppresses a form of replication-dependent
417 DNA damage that activates transcription of TERRA and associated small RNAs.
418 However, when small RNAs fail to promote heterochromatin formation at telomeres in
419 the absence of telomerase, our data suggest that EXO-1-mediated DNA damage then
420 leads to dysfunctional telomeres accompanied by high levels of TERRA that are
421 observed in early-generation *trt-1; dcr-1* double mutants (Figure 5). Importantly, loss of
422 EXO1 in telomerase-negative mice has been shown to extend lifespan and improve
423 organ maintenance by repressing ssDNA formation and the DNA damage response
424 (Schaetzlein et al., 2007), suggesting a conserved role for Exonuclease-1 in the
425 metazoan response to dysfunctional telomeres. It is possible that heterochromatin
426 creates a more compact telomere architecture that is resistant to nucleolytic attack by
427 EXO-1. Alternatively, damage signaling from eroding telomeres may recruit EXO-1 and
428 other DNA damage factors.
429
430 Our results demonstrating that high levels of TERRA are associated with telomere
431 instability might be consistent with a role for TERRA expression in the DNA damage
432 response as discussed by two recent studies. First, in mammals TERRA expression
433 occurs in response to a distinct form of telomeric damage - acutely deprotected, non-
434 replicating telomeres in the presence of telomerase – and is accompanied by production
435 of telomeric siRNAs that promote DNA damage response factor recruitment (Rossiello
436 et al., 2017). Second, a recent study in *S. cerevisiae* showed that increased TERRA
437 expression and persistent telomeric R-loops in telomerase mutants can repress
438 senescence by promoting recombination, indicating that increased levels of TERRA can
439 in some contexts be beneficial (Graf et al., 2017). Our observations that high levels of
440 TERRA are induced in telomerase negative small RNA mutants in response to EXO-1

441 (Figure 5), suggest that TERRA may be induced by or integral to a telomeric DNA
442 damage response.
443
444 We detected subtelomeric siRNAs that were dependent on Dicer and that interacted
445 with the Argonaute proteins WAGO-1 and HRDE-1 (Figure 3H), both of which promoted
446 telomere stability in the absence of telomerase. These Argonaute proteins are known to
447 be active in the germline and bind to RdRP-generated 22G RNAs that target
448 overlapping groups of transcripts, including genes, transposons and pseudogenes (Gu
449 et al., 2009). Moreover, WAGO-1 localizes to perinuclear P-granules (or germ
450 granules), where it could promote either transcriptional or post-transcriptional gene
451 silencing (Gu et al., 2009), whereas HRDE-1 is localized to the nucleus where it
452 promotes transcriptional gene silencing. The *C. elegans* Piwi homolog PRG-1 also
453 localizes to P granules, where it interacts with piRNAs to promote the biogenesis of
454 secondary 22G RNAs that may interact with HRDE-1 molecules that transiently enter P
455 granules before entering the nucleus to promote heterochromatin silencing. Moreover,
456 HRDE-1 and WAGO-1 have been shown to function redundantly to promote
457 transgenerational epigenomic silencing of transgenes, a form of permanent epigenomic
458 silencing that is initiated by PRG-1/Piwi and associated piRNAs (Ashe et al., 2012,
459 Buckley et al., 2012). Given that HRDE-1 and WAGO-1 interact with 22G siRNAs that
460 map to distinct and overlapping subtelomeres, we propose that these Argonaute
461 proteins collaborate to promote heterochromatin formation at subtelomeres, such that
462 both P-granule localized WAGO-1 and nuclear Argonaute HRDE-1 play important roles
463 in this silencing process. Although proteomics has been performed for both HRDE-1
464 and WAGO-1, these Argonaute proteins do not physically interact with one another or
465 possess common interacting proteins (Akay et al., 2017, Shirayama et al., 2014). We
466 propose that EXO-1-mediated telomere resection is accompanied by expression of
467 TERRA and ARRET, resulting in low levels of dsRNA that would elicit Dicer recruitment
468 via RDE-4 to create a primary siRNA population that would be amplified by RdRPs to
469 create 22G RNAs that associate with WAGO-1 and HRDE-1 to promote telomeric
470 silencing (Figure 6).
471

472 We did not detect any telomeric siRNAs lacking mismatches in our analysis of siRNAs
473 from telomerase mutants, nor could we identify Dicer-dependent telomeric siRNAs that
474 had mismatches. However, we did find that exogenous telomeric siRNAs were able to
475 complement the premature sterility of *trt-1 dcr-1* mutants (Figure 4A). Together, our
476 results suggest that while telomeric siRNAs can promote telomere stability in the
477 absence of telomerase, that subtelomeric transcripts are templates for *de novo*
478 synthesis of endogenous siRNAs that are relevant to telomere repeat stability.
479 Consistently, TERRA transcription in *S. pombe* initiates in the subtelomere but rarely
480 extends into the telomere (Moravec et al., 2016). We propose that TERRA is not
481 significantly expressed in RNAi deficient mutants that possess wildtype telomerase,
482 because telomerase is capable of healing telomeric damage that occurs in the absence
483 of small RNA-mediated heterochromatin formation.
484
485 Small RNAs promote genomic silencing of many types of transposons and are essential
486 for the stability of *Drosophila melanogaster* telomeres, which are composed of non-LTR
487 retrotransposons that are distinct from the simple repetitive sequences that are
488 maintained by telomerase and cap chromosome ends in most organisms (Pardue and
489 DeBaryshe, 2003). siRNAs function at *Drosophila* telomeres to promote
490 heterochromatin-mediated genome silencing via the *Drosophila* homologs of HP1 and
491 ATRX, thereby preventing telomere instability (Chavez et al., 2017, Fulcher et al.,
492 2014). Small RNA-mediated control of telomere stability through regulation of
493 heterochromatin is therefore a conserved feature of both non-canonical and canonical
494 telomeres. siRNA dysfunction at *Drosophila* telomeres leads to immediate telomere
495 deprotection and fusion in embryos, whereas *C. elegans* siRNA mutants telomeres
496 have normal lengths (Figure S1). When both telomerase and *C. elegans* siRNA factors
497 are removed, telomeres trigger a DNA damage response in many germ cells but this
498 does not result in telomere fusions for several generations, each generation
499 representing 8-10 cell divisions. This indicates that the accelerated sterility phenotype of
500 siRNA-deficient *trt-1* mutants is not a consequence of a defect in acute telomere
501 uncapping, but rather an acceleration of the onset of crisis. We speculate siRNA-
502 mediated heterochromatin formation at telomeres modulates the stability of telomeres in

503 diverse organisms that maintain their telomeres via telomerase-mediated telomere
504 repeat addition.
505
506 Since most human somatic cells do not express telomerase, our findings may be
507 generally relevant to understanding how cells control the rate of telomere shortening in
508 the absence of telomerase through modulation of telomeric transcription and chromatin
509 either in the germ cells, in the early embryo or in adult somatic cells. Increased TERRA
510 expression and telomeric R-loops have been reported to associate with high levels of
511 DNA damage in ICF syndrome cells, which are deficient for DNA methylation at
512 repetitive segments of the genome, including telomeres, and undergo rapid telomere
513 shortening and senescence (Sagie et al., 2017). As telomeric damage associated with
514 senescence can induce broad changes to chromatin and histone biosynthesis
515 (O'Sullivan et al., 2010), and our data suggest that the reverse may also be true; global
516 dysfunction of the epigenome, which may be a hallmark of human aging (Zhang et al.,
517 2015), could elicit rapid telomere instability and irreversible damage in cells that are
518 deficient for telomerase. We propose that small RNAs could be generally relevant to
519 lncRNA-mediated heterochromatin formation at telomeres and possibly elsewhere in the
520 genome, such as loci that are subjected to parent-of-origin genomic imprinting (Holoch
521 and Moazed, 2015, Taylor et al., 2015).
522
523 Finally, we note that the *C. elegans* secondary siRNA biogenesis factor MUT-7 (Figure
524 1A, B) is homologous to the exonuclease domain of human WRN1, which is commonly
525 mutated in Werner's syndrome and results in early-onset aging of multiple tissues.
526 WRN1 deficiency is accompanied by accelerated telomere erosion and senescence
527 phenotypes that can be rescued by telomerase expression (Shimamoto et al., 2015).
528 While WRN1 and its homologs have been intensively studied for their roles in DNA
529 recombination, WRN1 was recently shown to safeguard the epigenomic stability of
530 heterochromatin (Zhang et al., 2015). Our study suggests that Werner syndrome may
531 be explained, in part, by defects in siRNA-mediated heterochromatin silencing at
532 telomeres and elsewhere in the genome.
533

534
535
536
537 **Materials and Methods**
538
539 Strains: Unless otherwise noted, all strains were maintained at 20°C on nematode
540 growth medium plates seeded with *Escherichia coli* OP50. Strains used include Bristol
541 N2 ancestral, *wago-1(tm1414)*, *trt-1(ok410), unc-29(e193), dpy-5(e61), dcr-1(mg375),*
542 *hrde-1(tm1200), rde-1(ne219), rde-4(ne299), rrf-3(mg373), rrf-2(ok210), eri-1(mg366),*
543 *mut-7(pk204), mut-7(pk720), mut-14(pk738), rbr-2(tm1231), spr-5(by101), xnp-*
544 *1(ok1823), xnp-1(tm678), hpl-1(tm1624), hpl-2(ok916), hpl-2(tm1479), exo-1(tm1842)*.
545 A *trt-1 unc-29* double mutant, where *unc-29* is tightly linked to *trt-1*, was used to create
546 strains used in this study. Double, triple and quadruple mutants were created using
547 standard marker mutations and verified based on phenotype or genotype.

548 DAPI staining: One-day-old adults were washed twice in M9, soaked in 150 µL of
549 400ng/mL DAPI in ethanol solution for 30 min or until evaporated, rehydrated in 2 mL of
550 M9 solution overnight at 4°C, and mounted in 8 µL VECTASHIELD mounting medium
551 (Vector Laboratories). Chromosome counts were performed under 60x magnification
552 and a 359nm excitation wavelength using a Nikon Eclipse E800 microscope.

553 qPCR: Non-starved mixed-stage worms were washed with M9 and RNA was extracted
554 using 1 mL TRIZOL according to the manufacturer's instructions. For RT-PCR analysis,
555 total RNA was treated twice with DNase I and was reverse transcribed with act-1 and a
556 telomere-specific primer ($(GCCTAA)_3$) using SuperScript II reverse transcriptase
557 (Invitrogen). For SYBR green reactions, subtelomere specific primers were designed
558 within 200bp of the telomere-subtelomere junction.
559
560 RNA FISH: RNA FISH was performed as previously described (Sakaguchi et al., 2014)
561 with several modifications. In brief, non-starved, mixed-stage animals were washed
562 twice in M9 and three times in 1x DEPC-treated PBS. Worms were fixed in 1mL
563 fixation buffer (1x DEPC-treated PBS with 3.7% formaldehyde) for 45 min rotating at

room temperature then washed twice in 1mL 1x DEPC-treated PBS. Fixed animals were permeabilized overnight at 4°C in 70% ethanol in DEPC-treated H_2O, then washed in 1 mL wash buffer [10% (vol/vol) formamide in 2x RNases-free SSC]. Aliquots of each sample were removed prior to hybridization and treated with RNaseA for 1h at 37°C to ensure probe specificity to RNA. Hybridization was performed at 30°C overnight in 100 µL hybridization buffer (10% dextran sulfate, 2x RNase-free SSC, 10% deionized formamide, 50, 0.02% RNase-free BSA, 50 µg *E. coli* tRNA) with 1.25 µM probe. Cy5-labelled $(GCCTAA)_3$ probe was used to detect TERRA transcripts. Animals were washed twice with wash buffer, counterstained with 25 ng/mL DAPI for 30 min at room temperature, and mounted on glass slides in VECTASHIELD mounting medium (Vector Laboratories) before epifluorescence microscopy.

IF: IF was carried out as previously described (Phillips et al., 2009) by fixing dissected gonads of 1 day old adults in 2% PFA for 10 minutes followed by a 1 minute postfixation in methanol. Rabbit anti-pS/TQ (Cell Signaling Technology) was used at a 1:500 dilution and mouse anti-RNA:DNA hybrid S9.6 at 1:500 dilution. Stained gonads were counterstained with DAPI and mounted with VECTASHIELD (Vector laboratories) before epifluorescence microscopy.

RNAi: RNAi clone expressing dsRNA targeting *C. elegans* telomeres was constructed using NEB HiFi DNA assembly mix according to the manufacturer's instructions. 200 bp of telomeric repeats were amplified from cTel55x by PCR with 20 bp overlap to SpeI digested L4440. Correct constructs were transformed into HT115 and RNAi was performed as previously described (McMurchy et al., 2017).

Southern Blot: *C. elegans* genomic DNA was digested overnight with Hinf1 (New England Biolabs), separated on a 0.8% agarose gel at 1.5 V/cm, and transferred to a neutral nylon membrane (Hybond-N, GE Healthcare Life Sciences). A digoxigenin-labelled telomere probe was hybridized and detected as described (Ahmed and Hodgkin, 2000).

595 Mrt and ALT assays: When telomerase-deficient *trt-1(ok410) C. elegans* mutants are
596 passaged by using the standard Mortal Germline (Mrt) assay developed in our
597 laboratory, which involves passaging six L1 larval animals to fresh plates weekly, 100%
598 become sterile within 20–30 generations. When *trt-1(ok410)* strains are passaged
599 weekly by transferring a 1cm^2 chunk of agar populated with ≈200–400 animals, 10-20%
600 of the strains survive for hundreds of generations. Mantel-Cox Log Rank Analysis was
601 used to determine differences of transgenerational lifespan between strains. A z-test
602 was performed to compare proportion of ALT survivors in chunked strains.
603
604 RNA-seq: Animals were grown at 20°C on 100 mm NGM plates seeded with OP50
605 bacteria. Two biological replicates were prepared for each genotype. RNA was
606 extracted using Trizol (Ambion) followed by isopropanol precipitation. RNA samples
607 were treated with 20U RNA 5' polyphosphatase (Lucigen, RP8092H) for 30 minutes at
608 37°C to remove 5' triphosphate groups. Library preparation and sequencing was
609 performed at the UNC School of Medicine High-Throughput Sequencing Facility
610 (HTSF). RNA-seq libraries were prepared using the NEXTflex Small RNA Library Prep
611 Kit for Illumina (Bio Scientific). Libraries were sequenced on an Illumina HiSeq 2500 to
612 produce approximately twenty million 50 bp single-end reads per library.
613
614 Analysis of high throughput sequencing data: Publicly available RNA-seq datasets were
615 download from the Gene Expression Omnibus (https://www.ncbi.nlm.nih.gov/geo/) (see
616 table X for library information). Adapter trimming was performed as required using the
617 bbduk.sh script from the bbmap suite3 and custom scripts (Bushnell, 2016). Reads were
618 then filtered for 22G species or all species between 18 and 30 nucleotides in length
619 using a custom python script. Reads were then converted to fasta format and mapped
620 to the *C. elegans* genome (WS251) using bowtie (Langmead et al., 2009) with the
621 following options: -M 1 -v 0 -best -strata. Uniquely mapping siRNAs were detected by
622 replacing the -M 1 parameter with -m 1. To detect telomere-mapping sRNAs, reads
623 were mapped to seven repeats of perfect telomere sequence (TTAGGC), allowing for
624 zero mismatches. Unmapped reads were re-mapped to the telomere sequence, this
625 time allowing for one mismatch. This step was repeated to detect reads that map to

626 telomeres with two or three mismatches. Genes with differential siRNA abundance in *trt-*
627 *1* were identified using DESeq2 (Love et al., 2014). To detect changes in the
628 abundance of subtelomeric siRNAs in *trt-1* and *trt-1; dcr-1*, 22G reads mapping to the
629 2kb of sequence adjacent to the telomere were counted for each chromosome arm.
630 Counts were normalized by dividing by the total number of mapped reads for each
631 library. A pseudocount of 1 was added to each normalized value to avoid division by
632 zero errors. Replicates were averaged and the log2-fold change between mutant and
633 wild-type was calculated for each subtelomere. Analysis of sequencing data was
634 performed using the R statistical computing environment (Team, 2017). Genome
635 regions were visualized using the Gviz R package (Hahne and Ivanek, 2016).
636 Immunoprecipitation datasets were used in Figure 3G, H but were excluded from the
637 analysis shown in Figure 3D-F. To detected siRNAs targeting transposons, 22G reads
638 were mapped to the *C. elegans* transposon consensus sequences downloaded from
639 Repbase with bowtie, allowing for up to two mismatches.
640 ChIP-seq reads were mapped to the genome as fastq files as described above without
641 the size filtering step. Read coverage was calculated at each base using bedtools
642 (Quinlan and Hall, 2010). Coverage values were normalized by dividing by the number
643 of total mapped reads for each library and enrichment was calculated by dividing the
644 normalized coverage for I.P. libraries by the normalized coverage of their respective
645 input libraries.
646
647 Accession numbers: RNA-seq data reported in this study are available under the
648 accession number GEO: GSE111800.
649
650 **Acknowledgements**
651 We thank R. Dowen for technical advice with qRT-PCR, K. Billmyre for advice on
652 immunofluorescence, and members of the S.A. laboratory for critical review of the
653 manuscript. Some strains were provided by the Caenorhabditis Genetics Center, which
654 is funded by National Institutes of Health Office of Research Infrastructure Programs
655 (P40 OD010440). S.F., C.L. and S.A. were supported by National Institute of Health
656 grant R01 GM066228.

Competing Interests

The authors declare no competing interests.

660 **References**
661
662 AHMED, S. & HODGKIN, J. 2000. MRT-2 checkpoint protein is required for germline
663 immortality and telomere replication in *C. elegans*. *Nature,* 403**,** 159-64.
664 AKAY, A., DI DOMENICO, T., SUEN, K. M., NABIH, A., PARADA, G. E., LARANCE,
665 M., MEDHI, R., BERKYUREK, A. C., ZHANG, X., WEDELES, C. J., RUDOLPH,
666 K. L. M., ENGELHARDT, J., HEMBERG, M., MA, P., LAMOND, A. I.,
667 CLAYCOMB, J. M. & MISKA, E. A. 2017. The Helicase Aquarius/EMB-4 Is
668 Required to Overcome Intronic Barriers to Allow Nuclear RNAi Pathways to
669 Heritably Silence Transcription. *Dev Cell,* 42**,** 241-255 e6.
670 ARNOULT, N., VAN BENEDEN, A. & DECOTTIGNIES, A. 2012. Telomere length
671 regulates TERRA levels through increased trimethylation of telomeric H3K9 and
672 HP1alpha. *Nat Struct Mol Biol,* 19**,** 948-56.
673 ASHE, A., SAPETSCHNIG, A., WEICK, E. M., MITCHELL, J., BAGIJN, M. P.,
674 CORDING, A. C., DOEBLEY, A. L., GOLDSTEIN, L. D., LEHRBACH, N. J., LE
675 PEN, J., PINTACUDA, G., SAKAGUCHI, A., SARKIES, P., AHMED, S. & MISKA,
676 E. A. 2012. piRNAs Can Trigger a Multigenerational Epigenetic Memory in the
677 Germline of C. elegans. *Cell,* 150**,** 88-99.
678 AVGOUSTI, D. C., PALANI, S., SHERMAN, Y. & GRISHOK, A. 2012. CSR-1 RNAi
679 pathway positively regulates histone expression in C. elegans. *EMBO J,* 31**,**
680 3821-32.
681 AZZALIN, C. M. & LINGNER, J. 2015. Telomere functions grounding on TERRA firma.
682 *Trends Cell Biol,* 25**,** 29-36.
683 AZZALIN, C. M., REICHENBACH, P., KHORIAULI, L., GIULOTTO, E. & LINGNER, J.
684 2007. Telomeric repeat containing RNA and RNA surveillance factors at
685 mammalian chromosome ends. *Science,* 318**,** 798-801.
686 BAGIJN, M. P., GOLDSTEIN, L. D., SAPETSCHNIG, A., WEICK, E. M., BOUASKER,
687 S., LEHRBACH, N. J., SIMARD, M. J. & MISKA, E. A. 2012. Function, targets,
688 and evolution of Caenorhabditis elegans piRNAs. *Science,* 337**,** 574-8.
689 BATISTA, P. J., RUBY, J. G., CLAYCOMB, J. M., CHIANG, R., FAHLGREN, N.,
690 KASSCHAU, K. D., CHAVES, D. A., GU, W., VASALE, J. J., DUAN, S., CONTE,
691 D., JR., LUO, S., SCHROTH, G. P., CARRINGTON, J. C., BARTEL, D. P. &
692 MELLO, C. C. 2008. PRG-1 and 21U-RNAs interact to form the piRNA complex
693 required for fertility in C. elegans. *Mol Cell,* 31**,** 67-78.
694 BENETTI, R., GARCIA-CAO, M. & BLASCO, M. A. 2007. Telomere length regulates the
695 epigenetic status of mammalian telomeres and subtelomeres. *Nat Genet,* 39**,**
696 243-50.
697 BENETTI, R., SCHOEFTNER, S., MUNOZ, P. & BLASCO, M. A. 2008. Role of TRF2 in
698 the assembly of telomeric chromatin. *Cell Cycle,* 7**,** 3461-8.
699 BERNSTEIN, E., CAUDY, A. A., HAMMOND, S. M. & HANNON, G. J. 2001. Role for a
700 bidentate ribonuclease in the initiation step of RNA interference. *Nature,* 409**,**
701 363-6.
702 BILLI, A. C., FISCHER, S. E. & KIM, J. K. 2014. Endogenous RNAi pathways in C.
703 elegans. *WormBook***,** 1-49.
704 BUCKLEY, B. A., BURKHART, K. B., GU, S. G., SPRACKLIN, G., KERSHNER, A.,
705 FRITZ, H., KIMBLE, J., FIRE, A. & KENNEDY, S. 2012. A nuclear Argonaute

706 promotes multigenerational epigenetic inheritance and germline immortality.
707 *Nature,* 489**,** 447-51.
708 BUSHNELL, B. 2016. BBMap short-read aligner, and other bioinformatics tools.
709 http://sourceforge.net/projects/bbmap/.
710 CANZIO, D., LARSON, A. & NARLIKAR, G. J. 2014. Mechanisms of functional
711 promiscuity by HP1 proteins. *Trends Cell Biol,* 24**,** 377-86.
712 CAO, F., LI, X., HIEW, S., BRADY, H., LIU, Y. & DOU, Y. 2009. Dicer independent
713 small RNAs associate with telomeric heterochromatin. *RNA,* 15**,** 1274-81.
714 CHAVEZ, J., MURILLO-MALDONADO, J. M., BAHENA, V., CRUZ, A. K.,
715 CASTANEDA-SORTIBRAN, A., RODRIGUEZ-ARNAIZ, R., ZURITA, M. &
716 VALADEZ-GRAHAM, V. 2017. dAdd1 and dXNP prevent genome instability by
717 maintaining HP1a localization at Drosophila telomeres. *Chromosoma,* 126**,** 697-
718 712.
719 CHENG, C., SHTESSEL, L., BRADY, M. M. & AHMED, S. 2012. Caenorhabditis
720 elegans POT-2 telomere protein represses a mode of alternative lengthening of
721 telomeres with normal telomere lengths. *Proc Natl Acad Sci U S A,* 109**,** 7805-10.
722 CUSANELLI, E., ROMERO, C. A. & CHARTRAND, P. 2013. Telomeric noncoding RNA
723 TERRA is induced by telomere shortening to nucleate telomerase molecules at
724 short telomeres. *Mol Cell,* 51**,** 780-91.
725 DAS, P. P., BAGIJN, M. P., GOLDSTEIN, L. D., WOOLFORD, J. R., LEHRBACH, N. J.,
726 SAPETSCHNIG, A., BUHECHA, H. R., GILCHRIST, M. J., HOWE, K. L.,
727 STARK, R., MATTHEWS, N., BEREZIKOV, E., KETTING, R. F., TAVARE, S. &
728 MISKA, E. A. 2008. Piwi and piRNAs act upstream of an endogenous siRNA
729 pathway to suppress Tc3 transposon mobility in the Caenorhabditis elegans
730 germline. *Mol Cell,* 31**,** 79-90.
731 DONATE, L. E. & BLASCO, M. A. 2011. Telomeres in cancer and ageing. *Philos Trans*
732 *R Soc Lond B Biol Sci,* 366**,** 76-84.
733 FISCHER, S. E., MONTGOMERY, T. A., ZHANG, C., FAHLGREN, N., BREEN, P. C.,
734 HWANG, A., SULLIVAN, C. M., CARRINGTON, J. C. & RUVKUN, G. 2011. The
735 ERI-6/7 helicase acts at the first stage of an siRNA amplification pathway that
736 targets recent gene duplications. *PLoS Genet,* 7**,** e1002369.
737 FLYNN, R. L., COX, K. E., JEITANY, M., WAKIMOTO, H., BRYLL, A. R., GANEM, N.
738 J., BERSANI, F., PINEDA, J. R., SUVA, M. L., BENES, C. H., HABER, D. A.,
739 BOUSSIN, F. D. & ZOU, L. 2015. Alternative lengthening of telomeres renders
740 cancer cells hypersensitive to ATR inhibitors. *Science,* 347**,** 273-7.
741 FULCHER, N., DERBOVEN, E., VALUCHOVA, S. & RIHA, K. 2014. If the cap fits, wear
742 it: an overview of telomeric structures over evolution. *Cell Mol Life Sci,* 71**,** 847-
743 65.
744 GENT, J. I., LAMM, A. T., PAVELEC, D. M., MANIAR, J. M., PARAMESWARAN, P.,
745 TAO, L., KENNEDY, S. & FIRE, A. Z. 2010. Distinct phases of siRNA synthesis
746 in an endogenous RNAi pathway in C. elegans soma. *Mol Cell,* 37**,** 679-89.
747 GOU, L. T., DAI, P., YANG, J. H., XUE, Y., HU, Y. P., ZHOU, Y., KANG, J. Y., WANG,
748 X., LI, H., HUA, M. M., ZHAO, S., HU, S. D., WU, L. G., SHI, H. J., LI, Y., FU, X.
749 D., QU, L. H., WANG, E. D. & LIU, M. F. 2014. Pachytene piRNAs instruct
750 massive mRNA elimination during late spermiogenesis. *Cell Res,* 24**,** 680-700.

751 GRAF, M., BONETTI, D., LOCKHART, A., SERHAL, K., KELLNER, V., MAICHER, A.,
752 JOLIVET, P., TEIXEIRA, M. T. & LUKE, B. 2017. Telomere Length Determines
753 TERRA and R-Loop Regulation through the Cell Cycle. *Cell,* 170**,** 72-85 e14.
754 GREER, E. L., MAURES, T. J., HAUSWIRTH, A. G., GREEN, E. M., LEEMAN, D. S.,
755 MARO, G. S., HAN, S., BANKO, M. R., GOZANI, O. & BRUNET, A. 2010.
756 Members of the H3K4 trimethylation complex regulate lifespan in a germline-
757 dependent manner in C. elegans. *Nature,* 466**,** 383-7.
758 GU, W., SHIRAYAMA, M., CONTE, D., JR., VASALE, J., BATISTA, P. J., CLAYCOMB,
759 J. M., MORESCO, J. J., YOUNGMAN, E. M., KEYS, J., STOLTZ, M. J., CHEN,
760 C. C., CHAVES, D. A., DUAN, S., KASSCHAU, K. D., FAHLGREN, N., YATES,
761 J. R., 3RD, MITANI, S., CARRINGTON, J. C. & MELLO, C. C. 2009. Distinct
762 argonaute-mediated 22G-RNA pathways direct genome surveillance in the C.
763 elegans germline. *Mol Cell,* 36**,** 231-44.
764 HAHNE, F. & IVANEK, R. 2016. Visualizing Genomic Data Using Gviz and
765 Bioconductor. *Methods Mol Biol,* 1418**,** 335-51.
766 HAN, T., MANOHARAN, A. P., HARKINS, T. T., BOUFFARD, P., FITZPATRICK, C.,
767 CHU, D. S., THIERRY-MIEG, D., THIERRY-MIEG, J. & KIM, J. K. 2009. 26G
768 endo-siRNAs regulate spermatogenic and zygotic gene expression in
769 Caenorhabditis elegans. *Proc Natl Acad Sci U S A,* 106**,** 18674-9.
770 HEARD, E. & TURNER, J. 2011. Function of the sex chromosomes in mammalian
771 fertility. *Cold Spring Harb Perspect Biol,* 3**,** a002675.
772 HOLOCH, D. & MOAZED, D. 2015. RNA-mediated epigenetic regulation of gene
773 expression. *Nat Rev Genet,* 16**,** 71-84.
774 HOLOHAN, B., WRIGHT, W. E. & SHAY, J. W. 2014. Cell biology of disease:
775 Telomeropathies: an emerging spectrum disorder. *J Cell Biol,* 205**,** 289-99.
776 KETTING, R. F., FISCHER, S. E., BERNSTEIN, E., SIJEN, T., HANNON, G. J. &
777 PLASTERK, R. H. 2001. Dicer functions in RNA interference and in synthesis of
778 small RNA involved in developmental timing in C. elegans. *Genes Dev,* 15**,** 2654-
779 9.
780 KETTING, R. F., HAVERKAMP, T. H., VAN LUENEN, H. G. & PLASTERK, R. H. 1999.
781 Mut-7 of C. elegans, required for transposon silencing and RNA interference, is a
782 homolog of Werner syndrome helicase and RNaseD. *Cell,* 99**,** 133-41.
783 KNIGHT, S. W. & BASS, B. L. 2001. A role for the RNase III enzyme DCR-1 in RNA
784 interference and germ line development in Caenorhabditis elegans. *Science,*
785 293**,** 2269-71.
786 LANGMEAD, B., TRAPNELL, C., POP, M. & SALZBERG, S. L. 2009. Ultrafast and
787 memory-efficient alignment of short DNA sequences to the human genome.
788 *Genome Biol,* 10**,** R25.
789 LI, F., HUARTE, M., ZARATIEGUI, M., VAUGHN, M. W., SHI, Y., MARTIENSSEN, R. &
790 CANDE, W. Z. 2008. Lid2 is required for coordinating H3K4 and H3K9
791 methylation of heterochromatin and euchromatin. *Cell,* 135**,** 272-83.
792 LI, J. S., MIRALLES FUSTE, J., SIMAVORIAN, T., BARTOCCI, C., TSAI, J.,
793 KARLSEDER, J. & LAZZERINI DENCHI, E. 2017. TZAP: A telomere-associated
794 protein involved in telomere length control. *Science,* 355**,** 638-641.
795 LOVE, M. I., HUBER, W. & ANDERS, S. 2014. Moderated estimation of fold change
796 and dispersion for RNA-seq data with DESeq2. *Genome Biol,* 15**,** 550.

LOVEJOY, C. A., LI, W., REISENWEBER, S., THONGTHIP, S., BRUNO, J., DE LANGE, T., DE, S., PETRINI, J. H., SUNG, P. A., JASIN, M., ROSENBLUH, J., ZWANG, Y., WEIR, B. A., HATTON, C., IVANOVA, E., MACCONAILL, L., HANNA, M., HAHN, W. C., LUE, N. F., REDDEL, R. R., JIAO, Y., KINZLER, K., VOGELSTEIN, B., PAPADOPOULOS, N., MEEKER, A. K. & CONSORTIUM, A. L. T. S. C. 2012. Loss of ATRX, genome instability, and an altered DNA damage response are hallmarks of the alternative lengthening of telomeres pathway. *PLoS Genet,* 8**,** e1002772.

MACIEJOWSKI, J. & DE LANGE, T. 2017. Telomeres in cancer: tumour suppression and genome instability. *Nat Rev Mol Cell Biol,* 18**,** 175-186.

MAICHER, A., KASTNER, L., DEES, M. & LUKE, B. 2012. Deregulated telomere transcription causes replication-dependent telomere shortening and promotes cellular senescence. *Nucleic Acids Res,* 40**,** 6649-59.

MCMURCHY, A. N., STEMPOR, P., GAARENSTROOM, T., WYSOLMERSKI, B., DONG, Y., AUSSIANIKAVA, D., APPERT, A., HUANG, N., KOLASINSKA-ZWIERZ, P., SAPETSCHNIG, A., MISKA, E. A. & AHRINGER, J. 2017. A team of heterochromatin factors collaborates with small RNA pathways to combat repetitive elements and germline stress. *Elife,* 6.

MORAVEC, M., WISCHNEWSKI, H., BAH, A., HU, Y., LIU, N., LAFRANCHI, L., KING, M. C. & AZZALIN, C. M. 2016. TERRA promotes telomerase-mediated telomere elongation in Schizosaccharomyces pombe. *EMBO Rep,* 17**,** 999-1012.

O'SULLIVAN, R. J., KUBICEK, S., SCHREIBER, S. L. & KARLSEDER, J. 2010. Reduced histone biosynthesis and chromatin changes arising from a damage signal at telomeres. *Nat Struct Mol Biol,* 17**,** 1218-25.

ORTIZ, M. A., NOBLE, D., SOROKIN, E. P. & KIMBLE, J. 2014. A new dataset of spermatogenic vs. oogenic transcriptomes in the nematode Caenorhabditis elegans. *G3 (Bethesda),* 4**,** 1765-72.

PAK, J. & FIRE, A. 2007. Distinct populations of primary and secondary effectors during RNAi in C. elegans. *Science,* 315**,** 241-4.

PARDUE, M. L. & DEBARYSHE, P. G. 2003. Retrotransposons provide an evolutionarily robust non-telomerase mechanism to maintain telomeres. *Annu Rev Genet,* 37**,** 485-511.

PFEIFFER, V. & LINGNER, J. 2012. TERRA promotes telomere shortening through exonuclease 1-mediated resection of chromosome ends. *PLoS Genet,* 8**,** e1002747.

PHILLIPS, C. M., BROWN, K. C., MONTGOMERY, B. E., RUVKUN, G. & MONTGOMERY, T. A. 2015. piRNAs and piRNA-Dependent siRNAs Protect Conserved and Essential C. elegans Genes from Misrouting into the RNAi Pathway. *Dev Cell,* 34**,** 457-65.

PHILLIPS, C. M., MCDONALD, K. L. & DERNBURG, A. F. 2009. Cytological analysis of meiosis in Caenorhabditis elegans. *Methods Mol Biol,* 558**,** 171-95.

PHILLIPS, C. M., MONTGOMERY, B. E., BREEN, P. C., ROOVERS, E. F., RIM, Y. S., OHSUMI, T. K., NEWMAN, M. A., VAN WOLFSWINKEL, J. C., KETTING, R. F., RUVKUN, G. & MONTGOMERY, T. A. 2014. MUT-14 and SMUT-1 DEAD box RNA helicases have overlapping roles in germline RNAi and endogenous siRNA formation. *Curr Biol,* 24**,** 839-44.

843 PICKETT, H. A. & REDDEL, R. R. 2015. Molecular mechanisms of activity and
844 derepression of alternative lengthening of telomeres. *Nat Struct Mol Biol,* 22**,**
845 875-80.
846 PORRO, A., FEUERHAHN, S., DELAFONTAINE, J., RIETHMAN, H., ROUGEMONT, J.
847 & LINGNER, J. 2014. Functional characterization of the TERRA transcriptome at
848 damaged telomeres. *Nat Commun,* 5**,** 5379.
849 QUINLAN, A. R. & HALL, I. M. 2010. BEDTools: a flexible suite of utilities for comparing
850 genomic features. *Bioinformatics,* 26**,** 841-2.
851 REINHART, B. J. & BARTEL, D. P. 2002. Small RNAs correspond to centromere
852 heterochromatic repeats. *Science,* 297**,** 1831.
853 ROSSIELLO, F., AGUADO, J., SEPE, S., IANNELLI, F., NGUYEN, Q., PITCHIAYA, S.,
854 CARNINCI, P. & D'ADDA DI FAGAGNA, F. 2017. DNA damage response
855 inhibition at dysfunctional telomeres by modulation of telomeric DNA damage
856 response RNAs. *Nat Commun,* 8**,** 13980.
857 SAGIE, S., TOUBIANA, S., HARTONO, S. R., KATZIR, H., TZUR-GILAT, A.,
858 HAVAZELET, S., FRANCASTEL, C., VELASCO, G., CHEDIN, F. & SELIG, S.
859 2017. Telomeres in ICF syndrome cells are vulnerable to DNA damage due to
860 elevated DNA:RNA hybrids. *Nat Commun,* 8**,** 14015.
861 SAKAGUCHI, A., SARKIES, P., SIMON, M., DOEBLEY, A. L., GOLDSTEIN, L. D.,
862 HEDGES, A., IKEGAMI, K., ALVARES, S. M., YANG, L., LAROCQUE, J. R.,
863 HALL, J., MISKA, E. A. & AHMED, S. 2014. Caenorhabditis elegans RSD-2 and
864 RSD-6 promote germ cell immortality by maintaining small interfering RNA
865 populations. *Proc Natl Acad Sci U S A,* 111**,** E4323-31.
866 SAPETSCHNIG, A., SARKIES, P., LEHRBACH, N. J. & MISKA, E. A. 2015. Tertiary
867 siRNAs mediate paramutation in C. elegans. *PLoS Genet,* 11**,** e1005078.
868 SCHAETZLEIN, S., KODANDARAMIREDDY, N. R., JU, Z., LECHEL, A.,
869 STEPCZYNSKA, A., LILLI, D. R., CLARK, A. B., RUDOLPH, C., KUHNEL, F.,
870 WEI, K., SCHLEGELBERGER, B., SCHIRMACHER, P., KUNKEL, T. A.,
871 GREENBERG, R. A., EDELMANN, W. & RUDOLPH, K. L. 2007. Exonuclease-1
872 deletion impairs DNA damage signaling and prolongs lifespan of telomere-
873 dysfunctional mice. *Cell,* 130**,** 863-77.
874 SETH, M., SHIRAYAMA, M., GU, W., ISHIDATE, T., CONTE, D., JR. & MELLO, C. C.
875 2013. The C. elegans CSR-1 argonaute pathway counteracts epigenetic
876 silencing to promote germline gene expression. *Dev Cell,* 27**,** 656-63.
877 SHAY, J. W. 2016. Role of Telomeres and Telomerase in Aging and Cancer. *Cancer*
878 *Discov,* 6**,** 584-93.
879 SHIMAMOTO, A., YOKOTE, K. & TAHARA, H. 2015. Werner Syndrome-specific
880 induced pluripotent stem cells: recovery of telomere function by reprogramming.
881 *Front Genet,* 6**,** 10.
882 SHIRAYAMA, M., STANNEY, W., 3RD, GU, W., SETH, M. & MELLO, C. C. 2014. The
883 Vasa Homolog RDE-12 engages target mRNA and multiple argonaute proteins to
884 promote RNAi in C. elegans. *Curr Biol,* 24**,** 845-51.
885 STEINER, F. A., OKIHARA, K. L., HOOGSTRATE, S. W., SIJEN, T. & KETTING, R. F.
886 2009. RDE-1 slicer activity is required only for passenger-strand cleavage during
887 RNAi in Caenorhabditis elegans. *Nat Struct Mol Biol,* 16**,** 207-11.

TABARA, H., YIGIT, E., SIOMI, H. & MELLO, C. C. 2002. The dsRNA binding protein RDE-4 interacts with RDE-1, DCR-1, and a DExH-box helicase to direct RNAi in C. elegans. *Cell,* 109**,** 861-71.

TAYLOR, D. H., CHU, E. T., SPEKTOR, R. & SOLOWAY, P. D. 2015. Long non-coding RNA regulation of reproduction and development. *Mol Reprod Dev,* 82**,** 932-56.

TEAM, R. C. 2017. R: A language and environment for statistical computing. R Foundation for Statistical Computing, Vienna, Austria. https://www.R-project.org/.

TIJSTERMAN, M., KETTING, R. F., OKIHARA, K. L., SIJEN, T. & PLASTERK, R. H. 2002. RNA helicase MUT-14-dependent gene silencing triggered in C. elegans by short antisense RNAs. *Science,* 295**,** 694-7.

UDUGAMA, M., FT, M. C., CHAN, F. L., TANG, M. C., PICKETT, H. A., JD, R. M., MAYNE, L., COLLAS, P., MANN, J. R. & WONG, L. H. 2015. Histone variant H3.3 provides the heterochromatic H3 lysine 9 tri-methylation mark at telomeres. *Nucleic Acids Res,* 43**,** 10227-37.

VRBSKY, J., AKIMCHEVA, S., WATSON, J. M., TURNER, T. L., DAXINGER, L., VYSKOT, B., AUFSATZ, W. & RIHA, K. 2010. siRNA-mediated methylation of Arabidopsis telomeres. *PLoS Genet,* 6**,** e1000986.

WEDELES, C. J., WU, M. Z. & CLAYCOMB, J. M. 2013. Protection of germline gene expression by the C. elegans Argonaute CSR-1. *Dev Cell,* 27**,** 664-71.

WELKER, N. C., PAVELEC, D. M., NIX, D. A., DUCHAINE, T. F., KENNEDY, S. & BASS, B. L. 2010. Dicer's helicase domain is required for accumulation of some, but not all, C. elegans endogenous siRNAs. *RNA,* 16**,** 893-903.

WICKY, C., VILLENEUVE, A. M., LAUPER, N., CODOUREY, L., TOBLER, H. & MULLER, F. 1996. Telomeric repeats (TTAGGC)n are sufficient for chromosome capping function in Caenorhabditis elegans. *Proc Natl Acad Sci U S A,* 93**,** 8983-8.

WONG, L. H., MCGHIE, J. D., SIM, M., ANDERSON, M. A., AHN, S., HANNAN, R. D., GEORGE, A. J., MORGAN, K. A., MANN, J. R. & CHOO, K. H. 2010. ATRX interacts with H3.3 in maintaining telomere structural integrity in pluripotent embryonic stem cells. *Genome Res,* 20**,** 351-60.

ZELLER, P., PADEKEN, J., VAN SCHENDEL, R., KALCK, V., TIJSTERMAN, M. & GASSER, S. M. 2016. Histone H3K9 methylation is dispensable for Caenorhabditis elegans development but suppresses RNA:DNA hybrid-associated repeat instability. *Nat Genet,* 48**,** 1385-1395.

ZHANG, W., LI, J., SUZUKI, K., QU, J., WANG, P., ZHOU, J., LIU, X., REN, R., XU, X., OCAMPO, A., YUAN, T., YANG, J., LI, Y., SHI, L., GUAN, D., PAN, H., DUAN, S., DING, Z., LI, M., YI, F., BAI, R., WANG, Y., CHEN, C., YANG, F., LI, X., WANG, Z., AIZAWA, E., GOEBL, A., SOLIGALLA, R. D., REDDY, P., ESTEBAN, C. R., TANG, F., LIU, G. H. & BELMONTE, J. C. 2015. Aging stem cells. A Werner syndrome stem cell model unveils heterochromatin alterations as a driver of human aging. *Science,* 348**,** 1160-3.

934

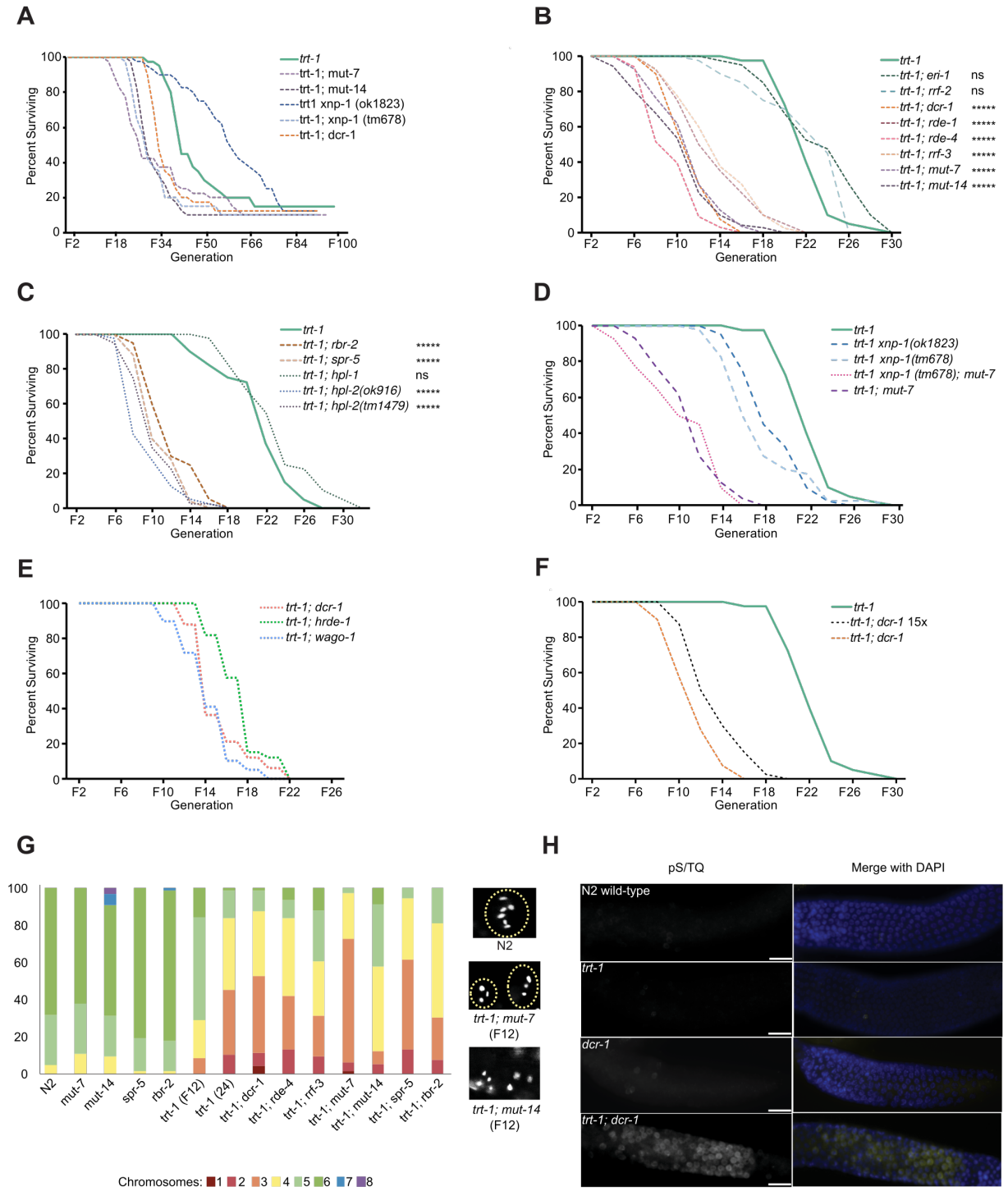

935

936 **Figure 1**: Endogenous small RNA and chromatin factors repress telomere stability in
937 the absence of telomerase. (A) Survival curve of telomerase-deficient strains passaged
938 at ~100 worms weekly for 40 independent lines. One allele of *xnp-1(ok1823)* extended
939 survival but did not increase survival via ALT (Table S1). (B) Survival curve of primary
940 or secondary siRNA deficient telomerase mutants when 6 larval L1s are passaged

941 weekly. (C) Survival curve of double mutants for *trt-1* and chromatin factors passaged
942 by 6 L1s weekly. (D) Histone H3.3 remodeling protein XNP-1 represses senescence in
943 *trt-1* mutants epistatically to the small RNA factor MUT-7. (E) Loss of HRDE-1 or
944 WAGO-1 Argonaute proteins mimics the accelerated sterility observed in a *trt-1; dcr-1*
945 mutant background. (F) A *trt-1; dcr-1* strain was crossed with *dcr-1* males fifteen times
946 to yield a *trt-1; dcr-1* 15x strain that displayed the same accelerated sterility observed
947 for the initial *trt-1; dcr-1* double mutants. (G) Small RNA and heterochromatin mutant *trt-*
948 *1* lines have high levels of chromosome fusions, comparable to *trt-1* single mutants at
949 F24. Fusions were assayed by diamidino-2-phenylindole (DAPI) staining of oocytes in
950 diakinesis. (H) High levels of phospho-(Ser/Thr) staining in the meiotic gonad of *trt-1;*
951 *dcr-1* at F6 compared to N2 or *trt-1*. Scale bar, 25mm. (B)-(D), (F) ***$p < 0.001$; ****$p <$
952 0.00001; ns, not significant, (Log rank test, n=40 independent lines for each genotype).
953 (E) *trt-1; wago-1* = 39 lines per genotype; *trt-1; hrde-1* and *trt-1; dcr-1* = 33 lines per
954 genotype.
955

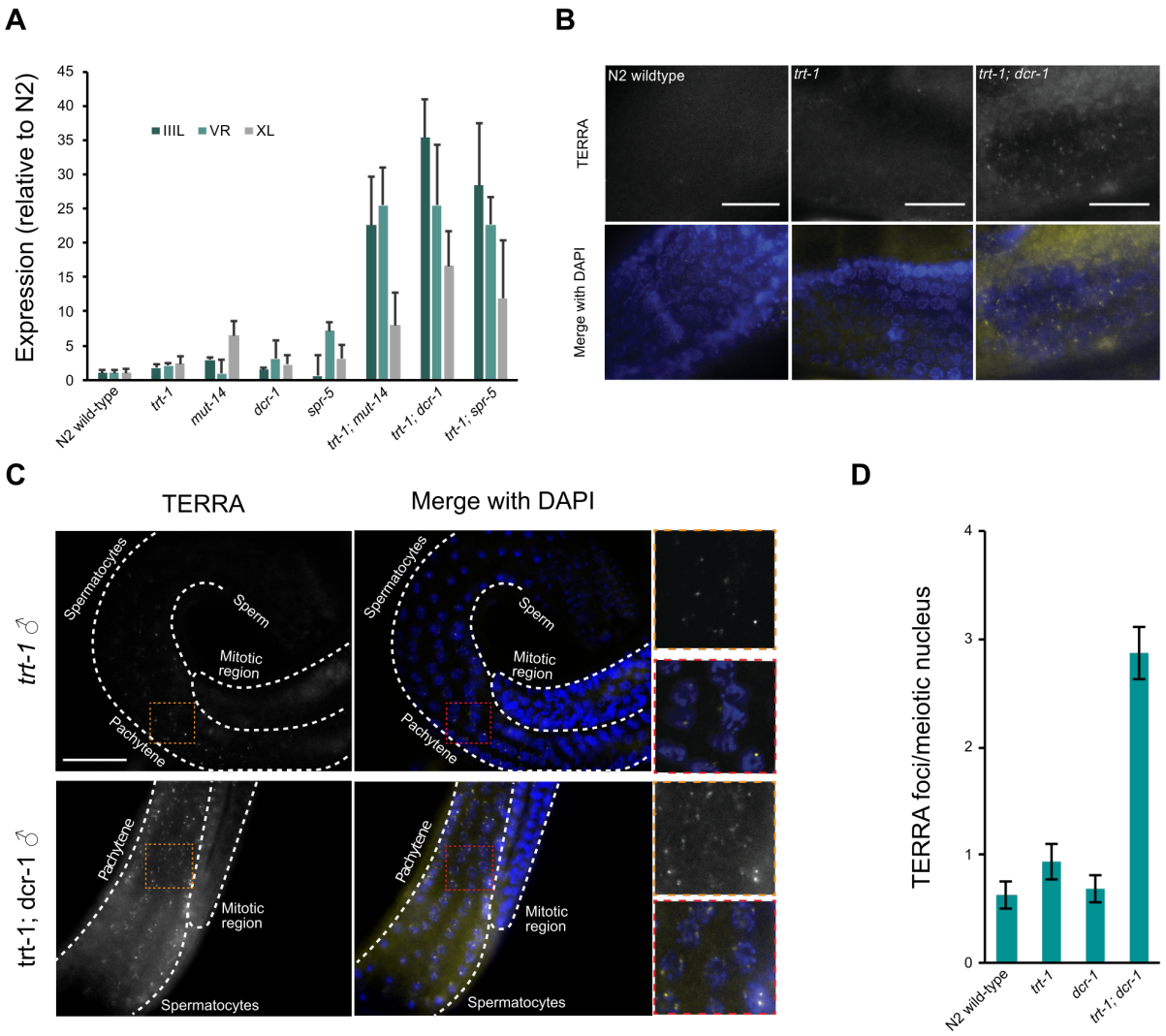

Figure 2: (A) Expression of TERRA from subtelomeres *IIIL*, *VR*, and *XL* is increased in siRNA and heterochromatin deficient telomerase mutants. cDNA was reverse transcribed with a telomere specific primer and qPCR was performed using subtelomere-specific primer pairs and normalized to *act-1*. Expression data are plotted relative to wildtype and represent the mean ± SEM of three biological replicates. (B) RNA FISH signals of TERRA in meiotic germlines of hermaphrodites of the indicated genotypes. TERRA foci are present in wildtype and *trt-1* in the pachytene region and increased in *trt-1; dcr-1.* Scale bar, 10um. (C) Representative RNA FISH images of TERRA in males show foci in the pachytene region of the germline which are increased in *trt-1; dcr-1* compared to *trt-1.* Scale bar, 20 um. (D) Quantification of germline TERRA foci (mean ± SEM, N=10 germlines).

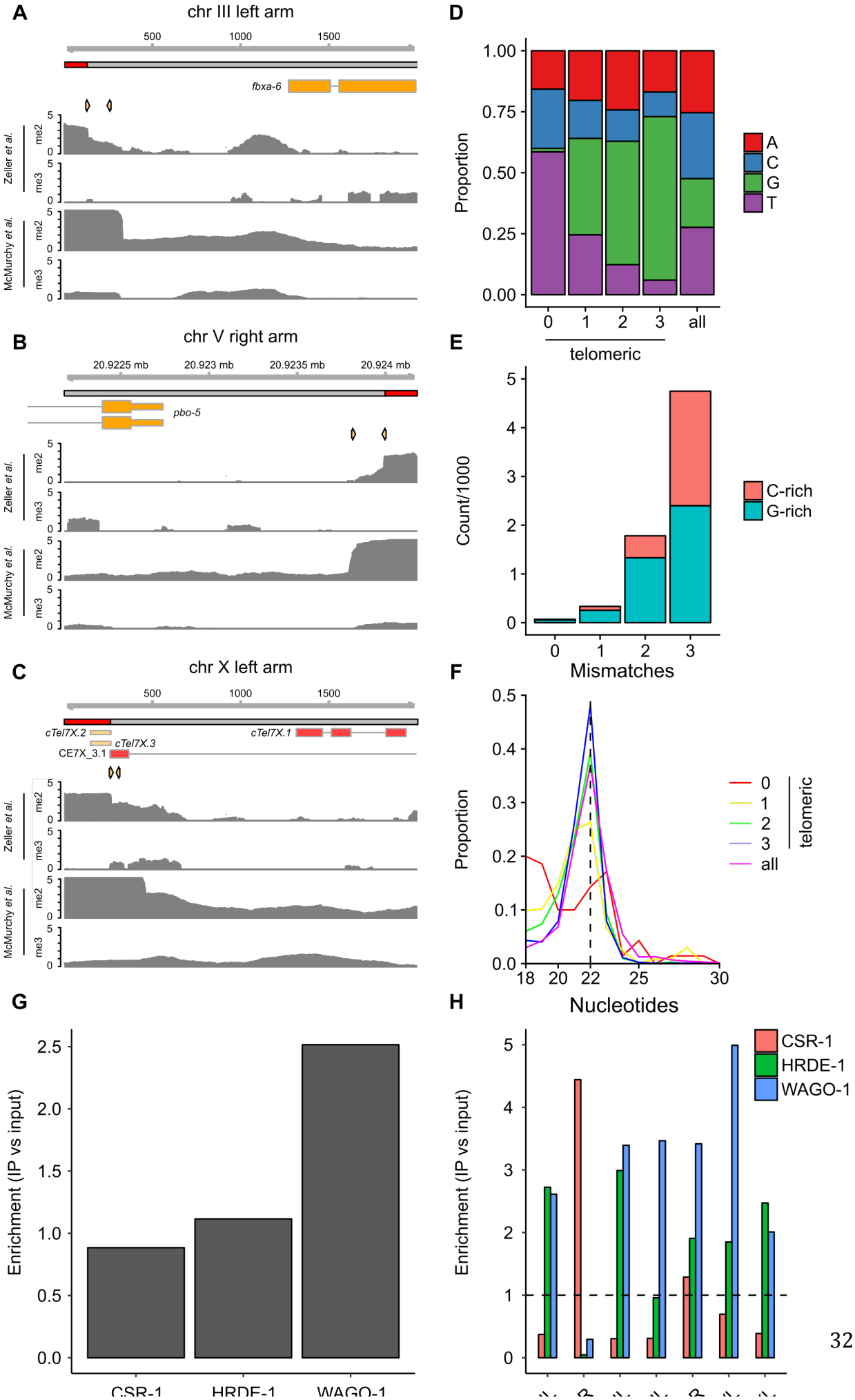
A
chr III left arm
500
1000
1500
fbxa-6
Zeller et al.
me2
me3
McMurchy et al.
B
chr V right arm
20.9225 mb
20.923 mb
20.9235 mb
20.924 mb
pbo-5
C
chr X left arm
cTel7X.2
cTel7X.3
CE7X_3.1
cTel7X.1
D
Proportion
A
C
G
T
0
1
2
3
all
telomeric
E
Count/1000
C-rich
G-rich
Mismatches
F
Proportion
Nucleotides
telomeric
G
Enrichment (IP vs input)
CSR-1
HRDE-1
WAGO-1
H
Enrichment (IP vs input)
CSR-1
HRDE-1
WAGO-1

971
972 **Figure 3:** Analysis of telomere-mapping small RNAs in published datasets. (A)-(C)
973 ChIP-seq enrichment profiles at three chromosome ends constructed using published
974 data (McMurchy et al., 2017, Zeller et al., 2016). Small orange arrows between gene
975 models and data tracks show the position of primers used in TERRA qRT-PCR
976 experiments. (D) Proportion of telomere-mapping small RNA reads in published data
977 beginning with a particular nucleotide. (E) Number of reads in published data mapping
978 to the G-rich (TTAGGC) or C-rich (GCCTAA) telomeric strand. (F) Distribution of small
979 RNA length in published data. (G) Enrichment (IP/input) of reads mapping to perfect
980 telomere sequence with up to three mismatches in published immunoprecipitation
981 datasets for three different Argonaute proteins. (H) Enrichment for subtelomeric siRNAs
982 for datasets used in (G). Numbers 0-3 in (D), (E) and (F) indicate number of
983 mismatches with perfect telomere.
984

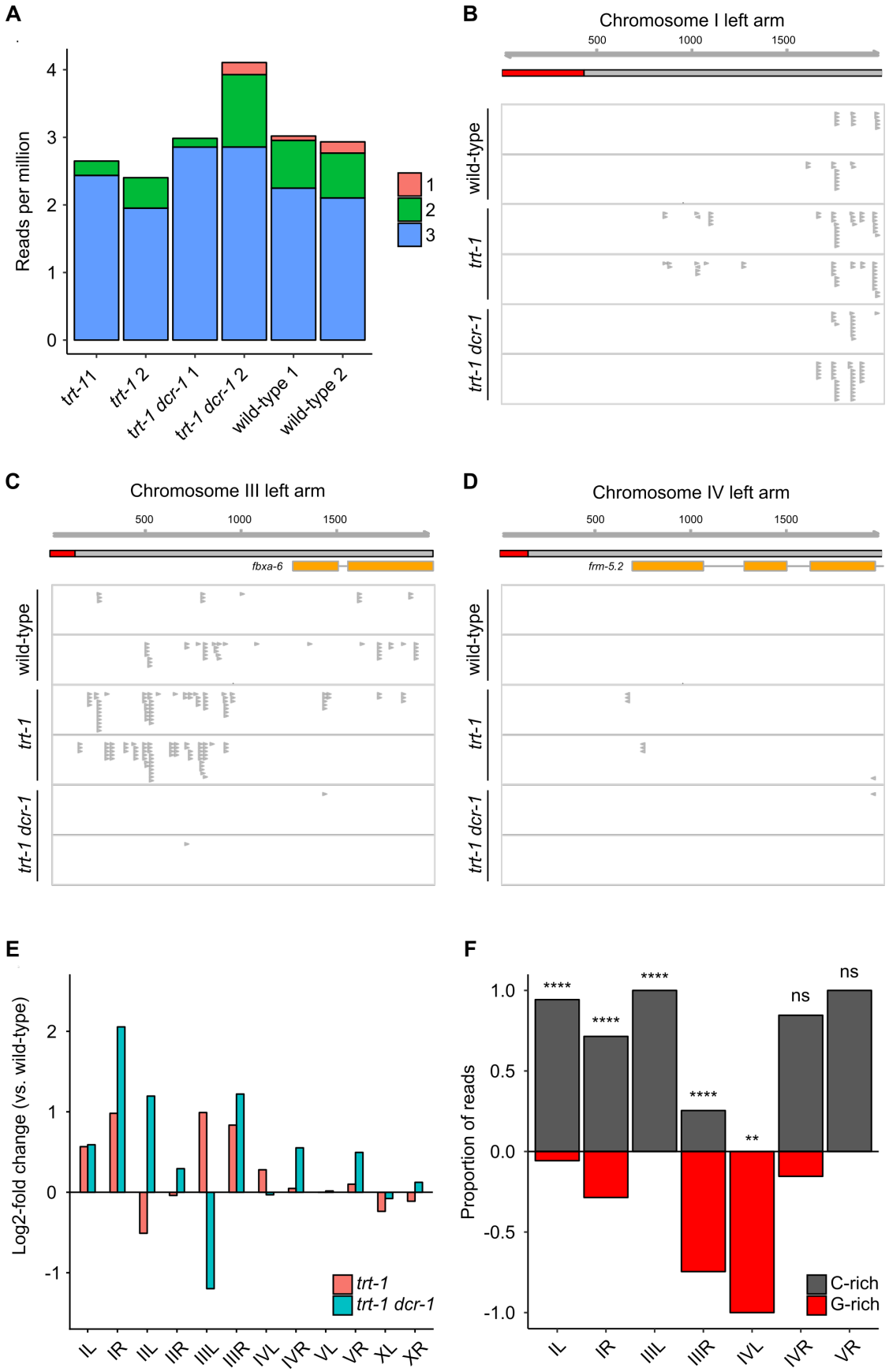
A
Reads per million
0
1
2
3
4
trt-1 1
trt-1 2
trt-1 dcr-1 1
trt-1 dcr-1 2
wild-type 1
wild-type 2
1
2
3
B
Chromosome I left arm
500
1000
1500
wild-type
trt-1
trt-1 dcr-1
C
Chromosome III left arm
500
1000
1500
fbxa-6
wild-type
trt-1
trt-1 dcr-1
D
Chromosome IV left arm
500
1000
1500
frm-5.2
wild-type
trt-1
trt-1 dcr-1
E
Log2-fold change (vs. wild-type)
-1
0
1
2
trt-1
trt-1 dcr-1
IL
IR
IIL
IIR
IIIL
IIIR
IVL
IVR
VL
VR
XL
XR
F
Proportion of reads
1.0
0.5
0.0
-0.5
-1.0
****
****
****
****
**
ns
ns
C-rich
G-rich
IL
IR
IIIL
IIIR
IVL
IVR
VR

985

986
987 **Figure 4:** Upregulation of subtelomeric siRNAs in telomerase mutants. (A) Number of
988 telomere-mapping reads in wild-type, *trt-1* and *trt-1;dcr-1* libraries. Numbers 1-3 indicate
989 number of mismatches. (B)-(D) 22G siRNAs at three subtelomeres. (E) Log2-fold
990 change in siRNA abundance at subtelomeres relative to wild-typein *trt-1* and *trt-1 dcr-1*
991 animals. (F) Proportion of subtelomeric siRNAs mapping to the strand corresponding to
992 the G-rich (TTAGGC) and C-rich (TAAGCC) telomere strand in *trt-1* animals. **** $p < 0.0001$; ** $p < 0.01$; ns, not significnat (Binomial test with Bonferroni correction).
994

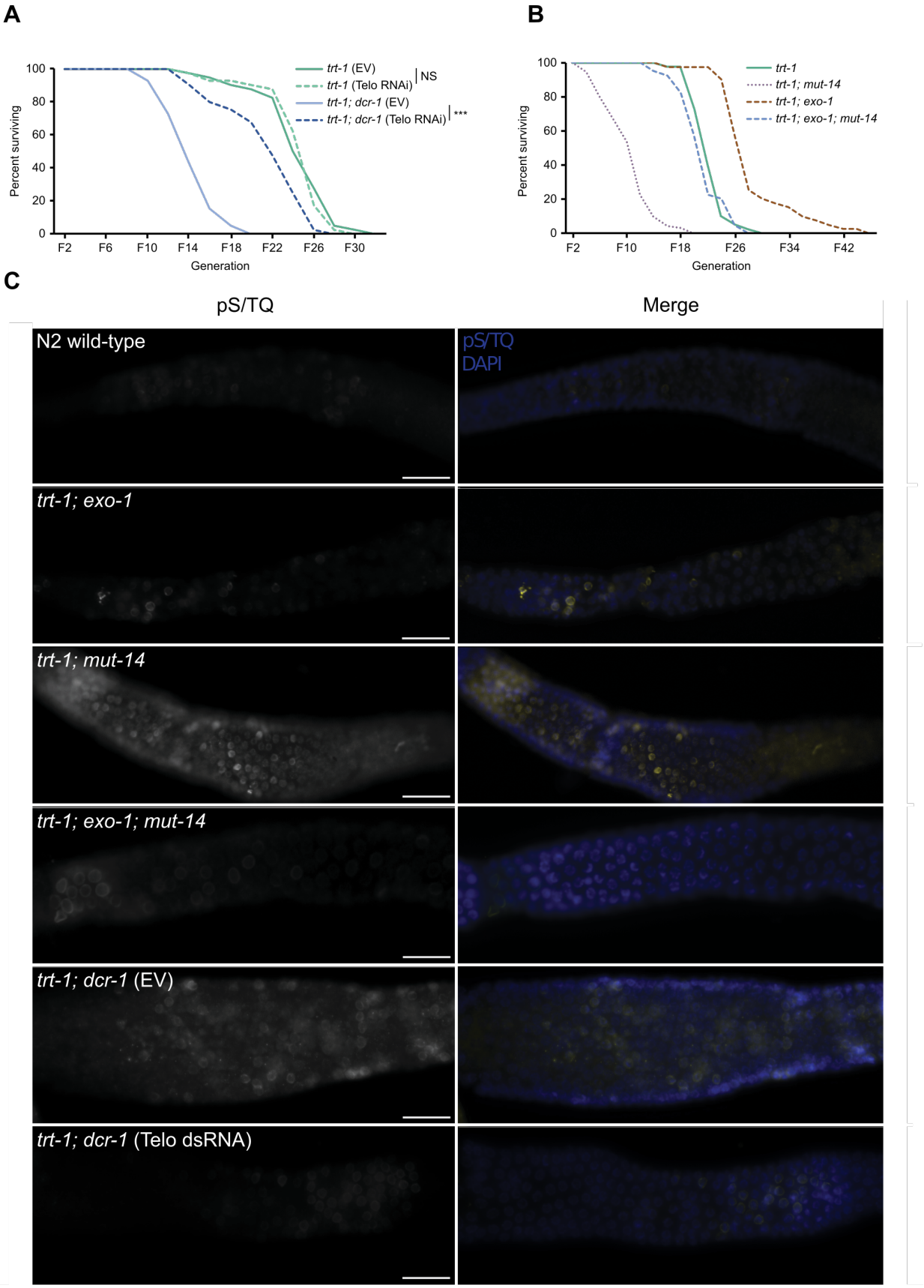
A
Percent surviving
Generation
trt-1 (EV)
trt-1 (Telo RNAi)
NS
trt-1; dcr-1 (EV)
trt-1; dcr-1 (Telo RNAi)
***
B
trt-1
trt-1; mut-14
trt-1; exo-1
trt-1; exo-1; mut-14
C
pS/TQ
Merge
N2 wild-type
pS/TQ
DAPI
trt-1; exo-1
trt-1; mut-14
trt-1; exo-1; mut-14
trt-1; dcr-1 (EV)
trt-1; dcr-1 (Telo dsRNA)

995

996
997 **Figure 5:** Fast senescence in siRNA-deficient *trt-1* is rescued by exogenous telomeric
998 dsRNA or loss of Exonuclease-1. (A) Survival of *trt-1* or *trt-1; dcr-1(mg375)* on either
999 empty vector control (EV) or bacteria expressing telomeric double-stranded RNA (telo
1000 dsRNA). Log rank test relative to EV, ***P < 0.001. n=40 lines per genotype. (B) Loss
1001 of *exo-1* extends survival of *trt-1; mut-14* lines. n=40 lines per genotype. (C) Telomeric
1002 dsRNA and loss of *exo-1* suppress accumulation of phospho-(Ser/Thr) in siRNA-
1003 deficient *trt-1* by F6. Scale bar=20um.
1004
1005
1006
1007

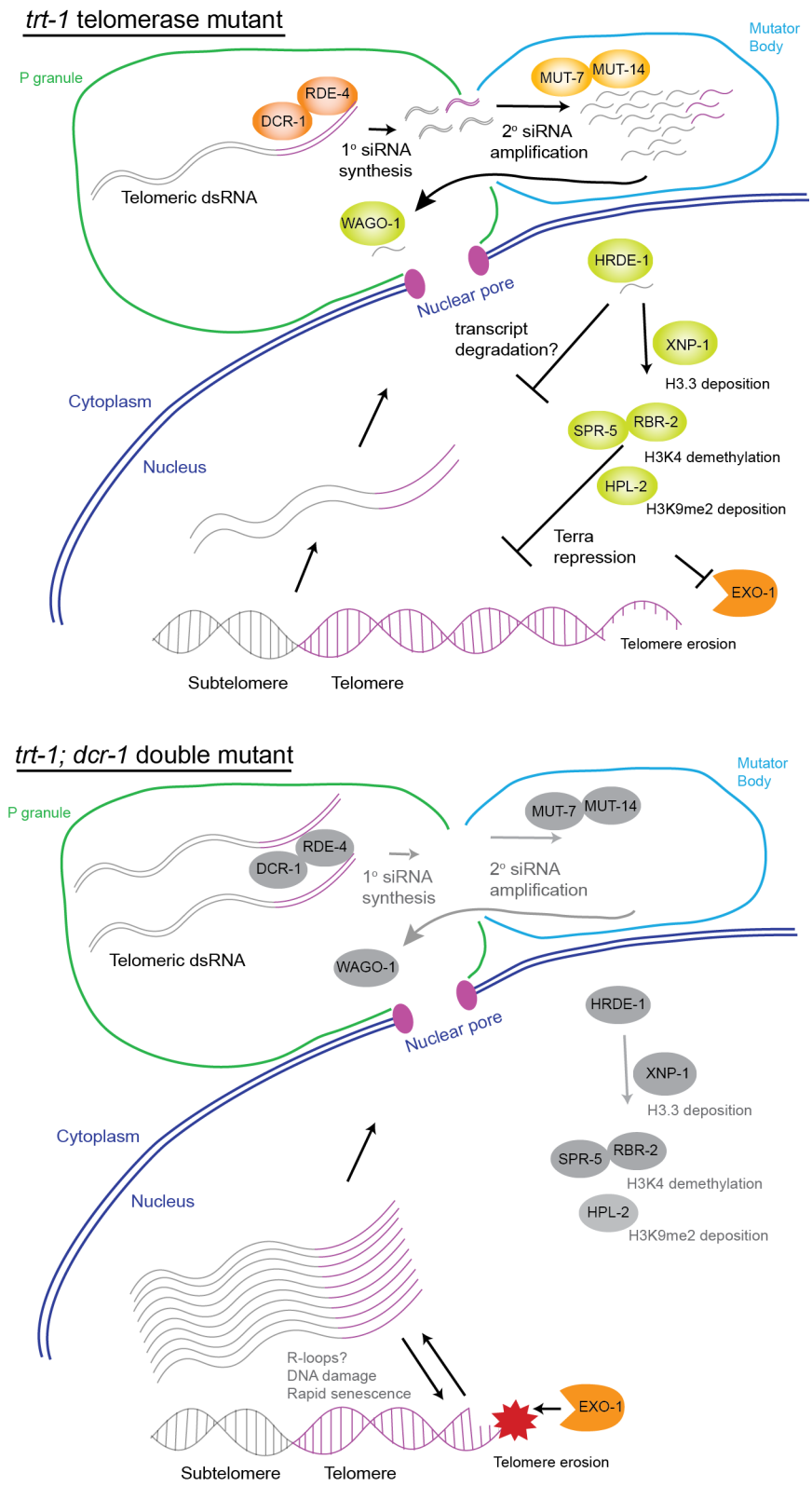

Figure 6: Model. In *trt-1* telomerase mutants, telomeric erosion induces expression of the lncRNA TERRA, which engages production of sub-telomeric and telomeric siRNAs.

Small RNAs promote deposition of H3K9me2 and H3K4 demethylation to maintain heterochromatic silencing of the telomere, repressing excess transcription, R-loop formation, DNA damage, and rapid senescence. In *trt-1; dcr-1* double mutants, TERRA expression is not repressed, leading to DNA damage, possibly RNA:DNA hybrids, and rapid senescence, which is dependent on the nuclease EXO-1.

Supplemental Information

5 Supplemental Figures

3 Supplemental Tables

1 Supplemental File

S1

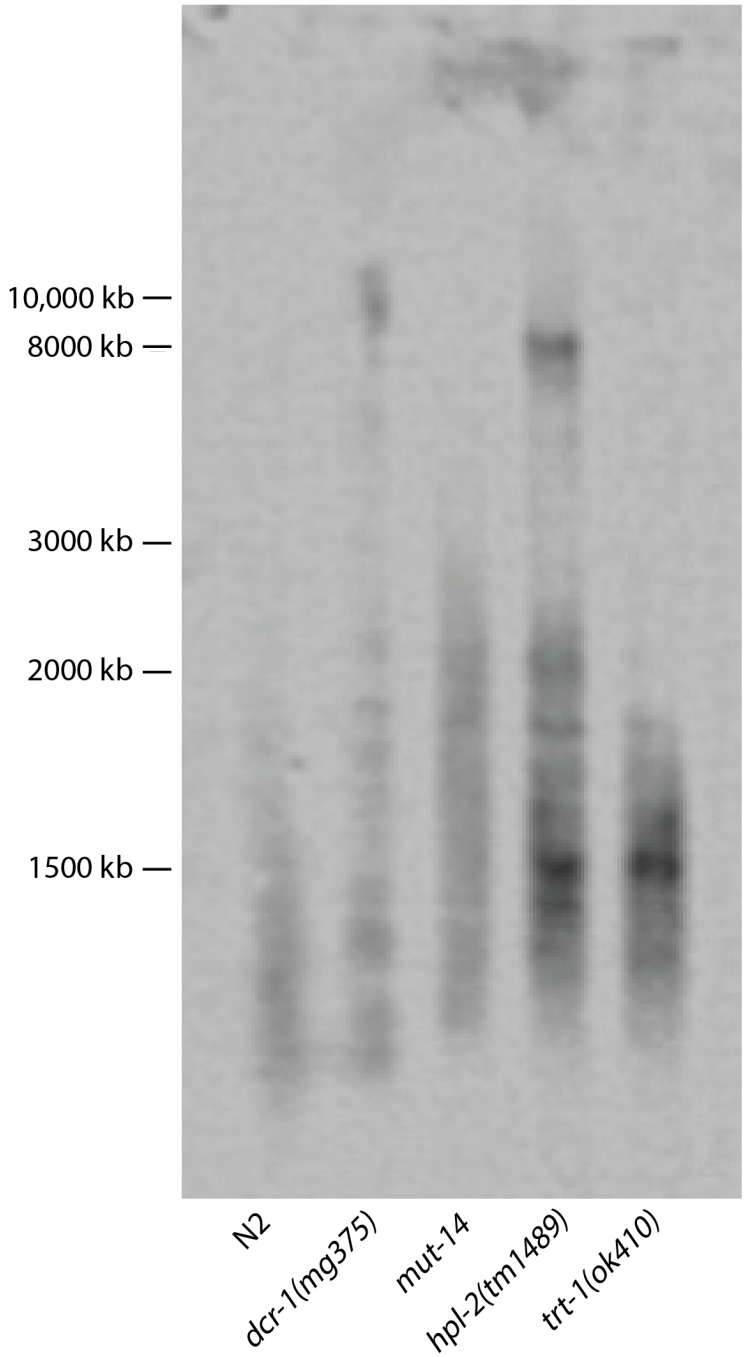

1034 **Figure S1. Related to Figure 1.** Terminal Restriction Fragment (TFR) analysis of
1035 wildtype and single mutant strains using a telomeric probe.

1036
1037
1038
1039
1040

S2

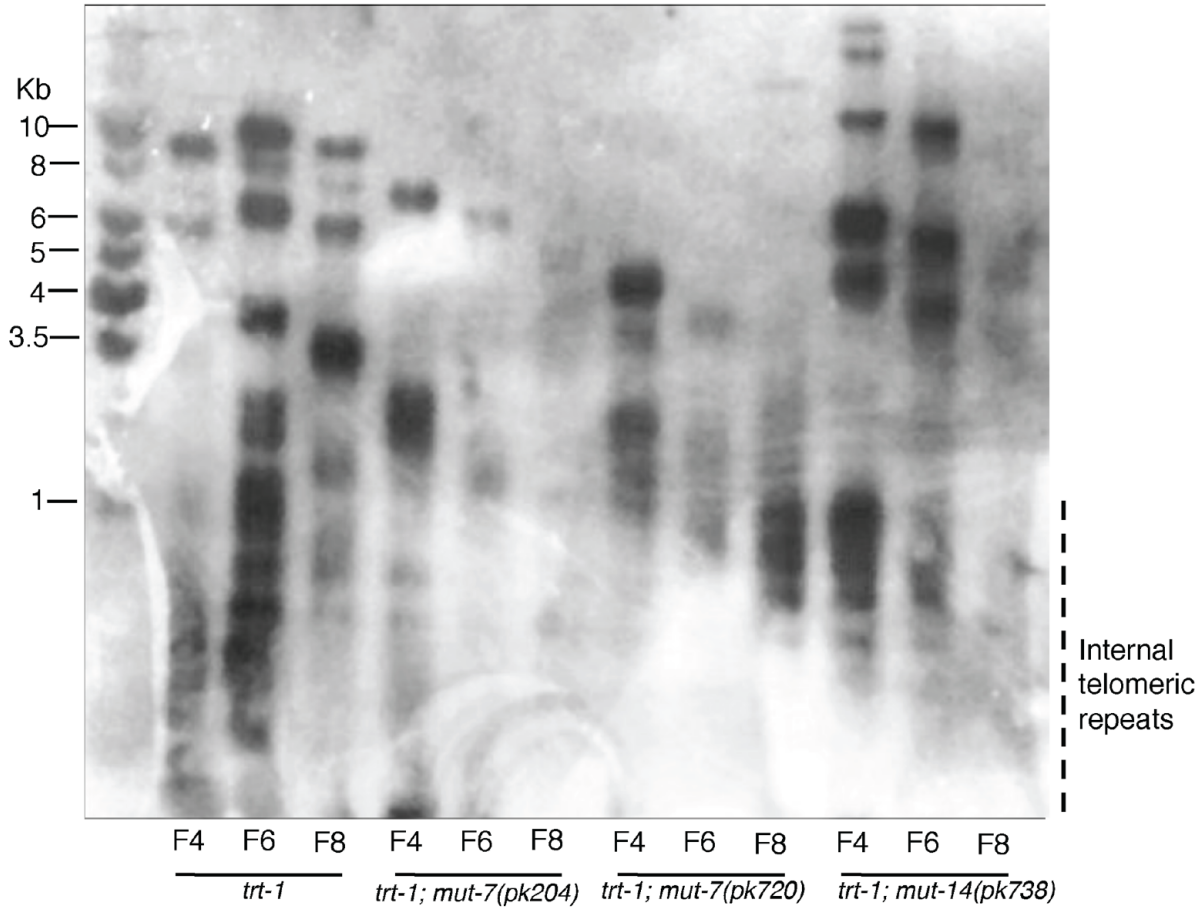

1041
1042
1043

1044 **Figure S2. Related to Figure 1.** TRF analysis of RNAi-deficient telomerase mutant
1045 strains using telomeric probe.

1046
1047

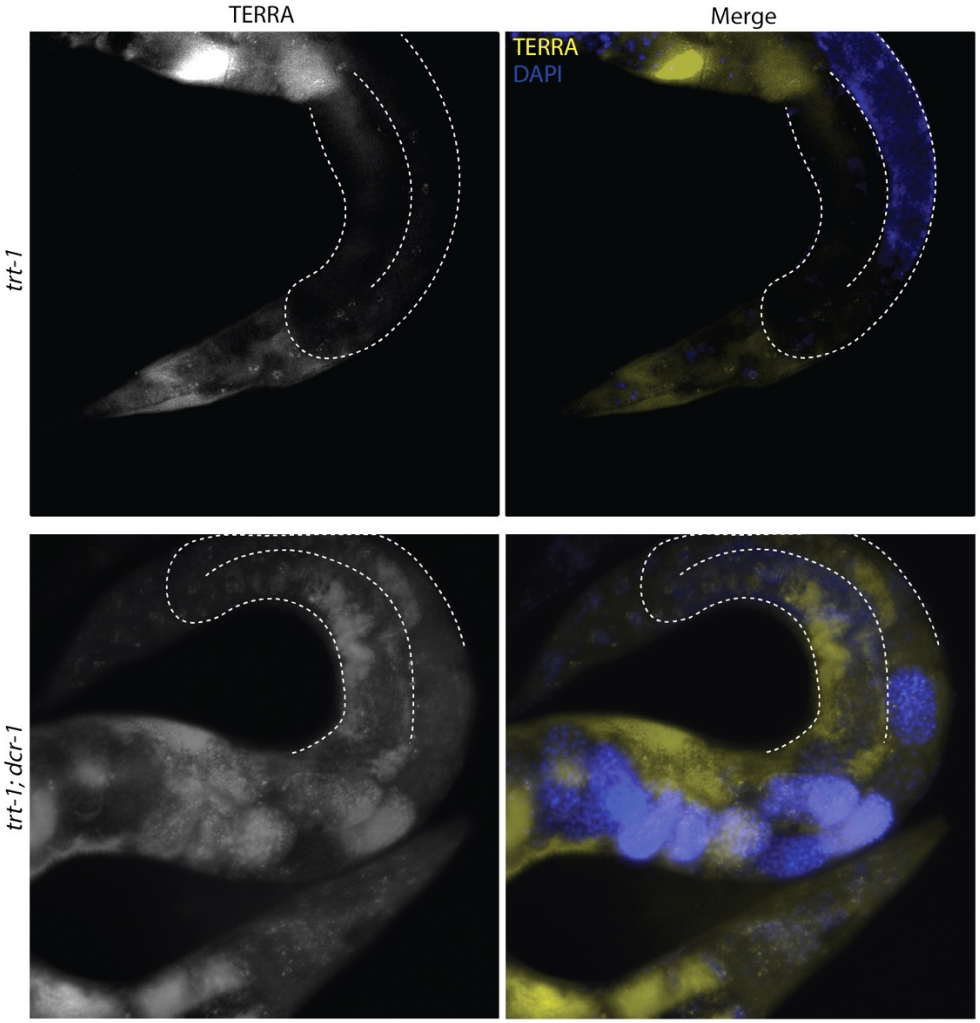

Figure S3. Related to Figure 2. TERRA expression (yellow) in *trt-1* and *trt-1; dcr-1(mg375)* 1 day old adults detected with a Cy5-labelled telomeric probe.

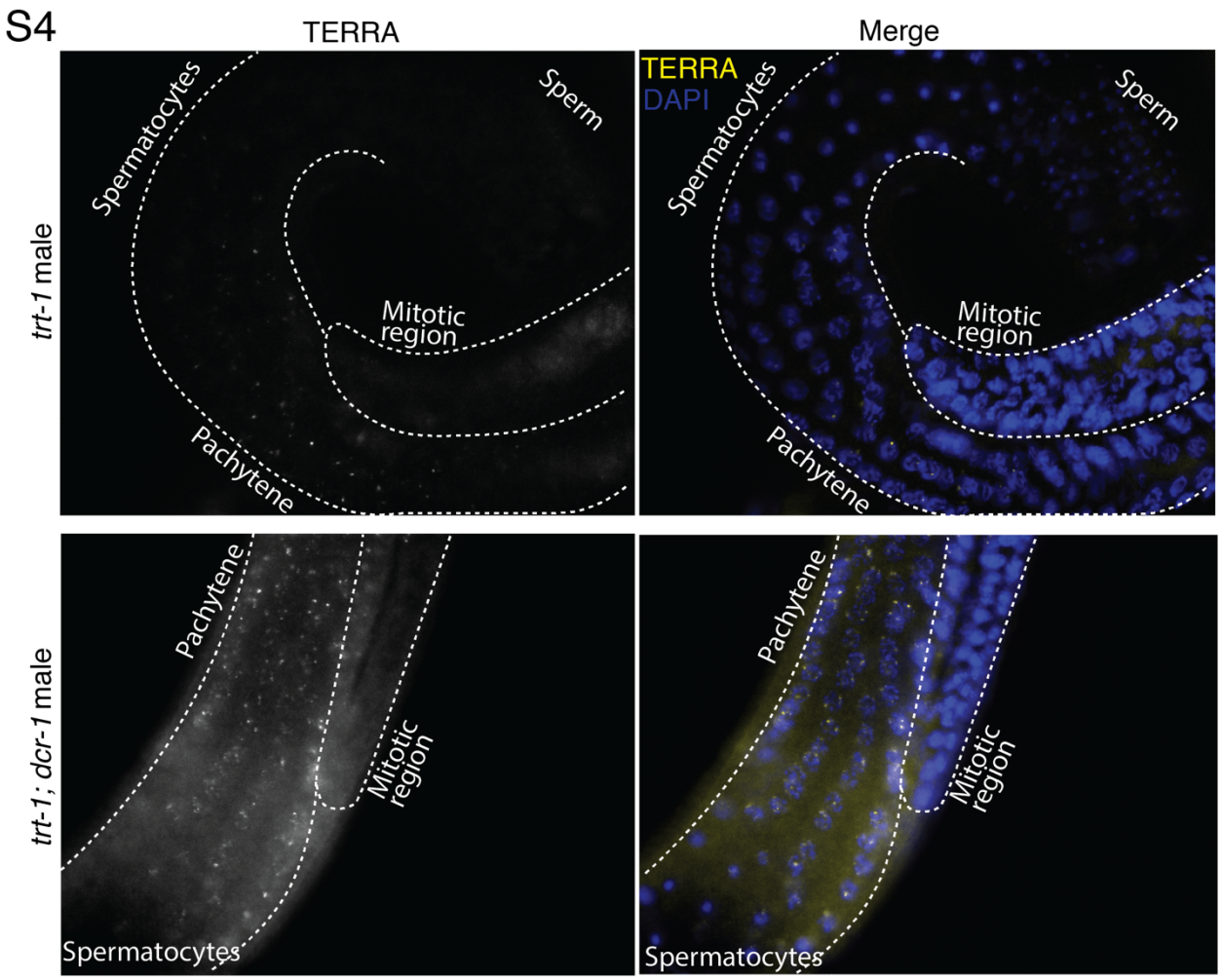

Figure S4. Related to Figure 2. RNA FISH of TERRA expression in *trt-1* and *trt-1; dcr-1* males. Note TERRA foci in the Pachytene region in both *trt-1* and *trt-1; dcr-1*, as well as lack of expression in the mitotic region and spermatocytes

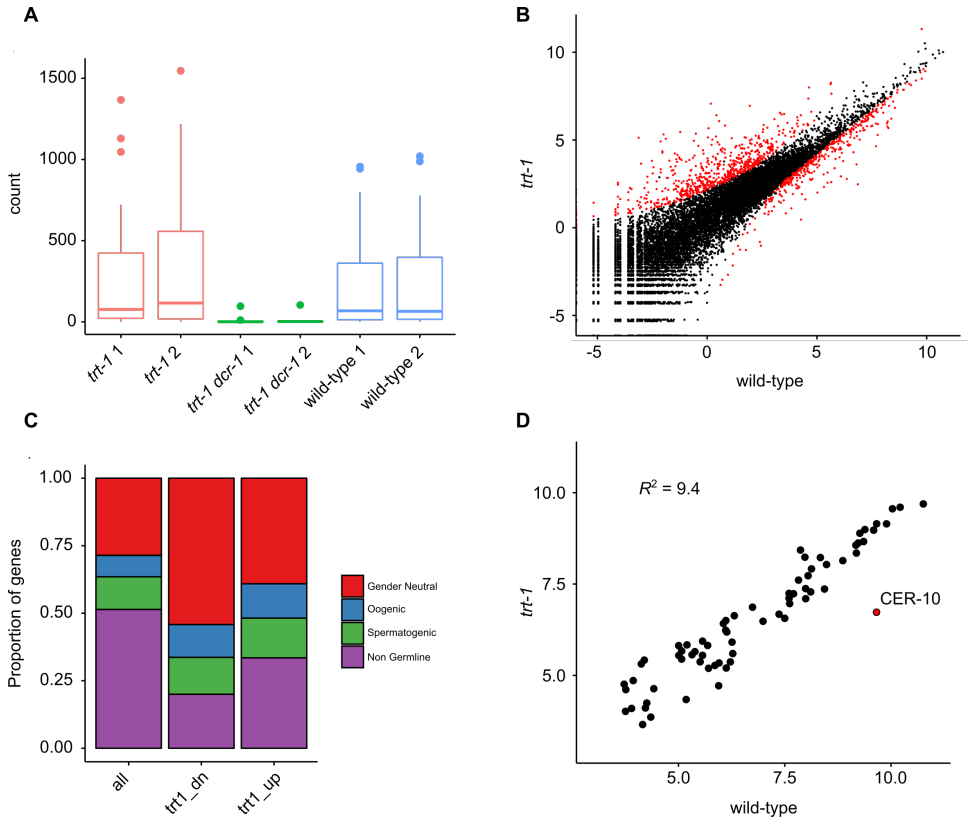

Figure S5. Related to Figure 3. Analysis of 22G small RNA species in telomerase and Dicer mutants. (A) Number of reads mapping to DCR-1 targets identified by Gent *et al.* (Gent et al., 2010). (B) log2 normalized mean read counts at every *C. elegans* gene for *trt-1* and wild-type. Genes identified as significantly differentially expressed by DESeq2 are shown in red. (C) Proportion of all genes or genes downregulated (trt1_dn) or upregulated (trt1_up) belonging to expression categories defined by Ortiz *et al.* (see reference 54 in main text). (D) log2 normalized mean read counts at transposon consensus sequences for *trt-1* and wild-type.

	Lines tested	Number ALT Survivors	Z score	p-value (two tailed)
trt-1	40	6		
trt-1; mut-7(pk204)	40	4	0.6761	0.4965
trt-1; mut-14(pk738)	40	4	0.6761	0.4965
trt-1 xnp-1(ok1823)	40	6	0	1
trt-1 xnp-1(tm678)	40	4	0.6761	0.4965
trt-1; dcr-1 (mg375)	40	5	0.3247	0.74896

Supplemental Table S1. Related to Figure 1. Statistical analysis of ALT survival strains. Loss of endogenous siRNA production (*mut-7*, *mut-14*, and *dcr-1*) or histone chaperone XNP-1/ATRX does not increase survival via ALT.

Strain	Log Rank test (Z=)	p-value
trt-1; mut-7(pk204)	9.79	<0.00001
trt-1; mut-14(pk738)	9.96	<0.00001
trt-1; dcr-1(mg375)	9.37	<0.00001
trt-1; rde-1	8.23	<0.00001
trt-1; rde-4	9.21	<0.00001
trt-1; rrf-3	8.4	<0.00001
trt-1; rrf-2	1.7	0.089
trt-1; exo-1	7.38	<0.00001
trt-1 xnp-1(ok1823)	4.3	<0.00001
trt-1 xnp-1(tm678)	4.23	<0.0001
trt-1 xnp-1(tm678); mut-7	9.21	<0.00001
trt-1; sid-1	6.52	<0.00001
trt-1; rbr-2(tm1231)	8.64	<0.00001
trt-1; spr-5 (by101)	8.89	<0.00001

Supplemental Table S2. Related to Figure 1. Log rank analysis of survival curves. N=40 independent lines for each genotype. Strains were passaged by transferring 6 larval L1s weekly and scored as sterile when plates contained no new L1 larvae.

1175
1176

trt-1 F1	males	dead embryos	*trt-1; dcr-1* F1	males	dead embryos
A1	13	6	A1	0	0
A2	4	26	A2	0	0
A3	8	24	A3	1	0
D1	10	11	A4	0	0
D2	11	4	B1	0	0
D3	4	9	B2	0	0
D4	13	15	B3	0	0
			B4	0	0
			C1	0	0
			C2	0	6
			C3	1	0
			C4	0	0
			D1	0	0
			D2	0	0
			D3	0	0
			D4	0	0

1177
1178
1179
1180 **Supplemental Table S3. Related to Figure 1.** Counts of total F2 males and dead
1181 embryos scored for F1 progeny from crosses of wildtype males with either late-
1182 generation F16 *trt-1* mutant controls (n=2 independently grown strains, three F1 scored
1183 for strain A and four F1 for strain D) or early generation F4 *trt-1; dcr-1* double mutant
1184 (n=4 strains, 4 F1 each scored for strains A, B, C and D) hermaphrodites. If a
1185 chromosome fusion is present in any of the F1 animals, then it will cause weak non-
1186 disjunction of the fused chromosomes, which leads to F2 dead embryos if an autosome
1187 is fused or to F2 males if the X chromosome is fused.
1188
1189
1190 **Supplemental File 1. Related to Figure 3.** Levels of telomeric siRNAs from wild-type
1191 and those of small RNA mutants.